



Distribution pattern of tumor infiltrating lymphocytes and tumor microenvironment composition as prognostic indicators in anorectal malignant melanoma

So-Woon Kim^{1,2} · Young Il Kim³ · Bilal Mustafa⁴ · Mi-Ju Kim⁵ · Gowun Jeong⁶ · Sung-Min Ahn⁷ · Seok-Byung Lim³ · Chang Sik Yu³ · Jin Cheon Kim³ · Seung-Mo Hong¹ · In Ja Park³

Received: 7 April 2020 / Revised: 15 July 2020 / Accepted: 15 July 2020 / Published online: 24 July 2020

© The Author(s), under exclusive licence to United States & Canadian Academy of Pathology 2020

Abstract

Anorectal malignant melanoma (ARMM) is a rare disease with poor prognosis. Determining ARMM prognosis precisely is difficult due to the lack of proper assessment techniques. Immunotherapy has proven effective against cutaneous malignant melanoma and may show efficacy in ARMM. Herein, we assessed the immune profile of ARMM to identify possible prognostic biomarkers. Twenty-two ARMM formalin-fixed and paraffin-embedded samples were evaluated using an nCounter[®] PanCancer Immune Profiling Panel. Validation was performed through immunohistochemical staining for CD3, CD8, Foxp3, CD68, CD163, and PD-L1. RNA analysis revealed significantly decreased scores for pathways involved in cell regulation and function, as well as chemokines, in recurrent patients compared to nonrecurrent patients. In cell-type profiling, the recurrent cases displayed significantly low tumor infiltrating lymphocyte (TIL) scores. Recurrence/death prediction models were defined using logistic regression and showed significantly lower scores in recurrent and deceased patients (all, $P < 0.001$) compared to those in nonrecurrent and surviving patients. The high total TIL and tumor-associated macrophage (TAM) groups had significantly better overall survival outcomes compared to the low total TIL and TAM groups ($P = 0.007$ and $P = 0.035$, respectively). In addition, the presence of CD3 + TILs in the invasion front was an independent favorable prognostic indicator ($P = 0.003$, hazard ratio = 0.21, 95% confidential interval, 0.01–0.41). Patients with inflamed or brisk-infiltration type tumors also had a significantly better overall survival than that of patients with immune-desert/excluded and absent/non-brisk type tumors ($P = 0.03$ and $P = 0.0023$, respectively). In conclusion, TILs have a strong prognostic value in ARMM, and the quantification of TILs and an analysis of the TIL phenotype and infiltration pattern during pathological diagnosis are essential to guide treatment strategies and accurate prognosis in ARMM.

These authors contributed equally: So-Woon Kim, Young Il Kim

Supplementary information The online version of this article (<https://doi.org/10.1038/s41379-020-0633-x>) contains supplementary material, which is available to authorized users.

✉ Seung-Mo Hong
smhong28@gmail.com

✉ In Ja Park
ipark@amc.seoul.kr

¹ Department of Pathology, Asan Medical Center, University of Ulsan College of Medicine, Seoul, Republic of Korea

² Department of Pathology, Kyung Hee University Hospital, Kyung Hee University College of Medicine, Seoul, Republic of Korea

³ Department of Colon and Rectal Surgery, Asan Medical Center, University of Ulsan College of Medicine, Seoul, Republic of Korea

Introduction

Anorectal malignant melanoma (ARMM) is a rare malignant mucosal disease that accounts for 1.3% of all malignant melanomas and 1% of anorectal malignant tumors [1].

⁴ Department of Health Sciences and Technology, Gachon Advanced Institute for Health Sciences and Technology, Gachon University, Incheon, Republic of Korea

⁵ Asan Institute for Life Sciences, Asan Medical Center, Seoul, Republic of Korea

⁶ Data Machine Intelligence Group, AI Center, SK Telecom, Seoul, Republic of Korea

⁷ Department of Genome Medicine and Science, College of Medicine, Gachon University, Incheon, Republic of Korea

The prognosis for ARMM is poor due to the unclear presentation of symptoms, and the 5-year survival rate of ARMM is only 10% [1–3]. Unlike those with cutaneous malignant melanoma, patients with ARMM are often only diagnosed when the disease is at an advanced stage, presenting clear symptoms, including rectal bleeding, pain, tenesmus, and obstruction, all of which often lead to disease misdiagnosis [4]. In addition, ARMMs are not caused by exposure to ultraviolet rays and are not always pigmented [2]. The pathogenesis of ARMM is still unknown, and it displays similar characteristics to those of cutaneous malignant melanoma; however, several studies have now reported a less frequent mutational burden and a higher proportion of structural chromosomal variants in ARMM [5–7]. Previous findings at the molecular level have indicated a lower number of *BRAF* gene mutations in mucosal malignant melanoma than in cutaneous malignant melanoma [8–13].

Immunotherapy is currently changing the landscape of treatment of malignant melanomas [14, 15]; surgical resection has limited effects on improving ARMM patient prognosis [16]. Clinical studies on the use of immunotherapy for mucosal malignant melanoma have demonstrated both promise and some limitations. For example, the objective response rate (ORR) of immunotherapy was found, in a number of studies, to be lower in advanced mucosal malignant melanoma compared to that in cutaneous malignant melanoma [17–19]. The median overall survival (OS) was also reported in the same studies to be significantly shorter in patients with mucosal malignant melanoma (11.3 months) than in those with cutaneous malignant melanoma (23.5 months) [17–19]. In contrast, patients with metastatic mucosal malignant melanoma have benefitted from treatment with the same immunotherapy regimens routinely used for patients with cutaneous malignant melanoma, with some patients having achieved durable and long-lasting responses [15, 17–19]. Furthermore, a study reported that immunotherapy in patients with unresectable and/or metastatic mucosal malignant melanomas yielded increased ORR and progression-free survival rates that were comparable to those in patients with cutaneous malignant melanoma, with no significant differences in the types of mucosal involvement [20]. These results suggest that an immune reaction occurs in patients with mucosal malignant melanoma receiving immunotherapy and that immunotherapy can be effective in these patients if correctly directed.

A few studies have suggested that tumor infiltrating lymphocytes (TILs) and programmed death-ligand 1 (PD-L1) are potential prognostic indicators in ARMM. Kaunitz et al. evaluated 36 mucosal malignant melanomas, including 3 ARMM cases, and observed a positive PD-L1 expression rate of 44%, which was similar to that in cutaneous malignant melanomas and was associated with a moderate to severe CD8 + TIL

expression [21]. Dodds et al. also observed a PD-L1 positivity rate of 44% among 43 ARMMs but reported that only 10% of the tumor cells were PD-L1 positive in 90% of the lesions [22]. Of note, these authors did not conduct a detailed evaluation of the immune contexts of the tumor microenvironment or their relationship with ARMM patient survival, which could provide some guidance in ARMM immunotherapy.

The aim of the present study was thus to analyze the clinicopathologic characteristics, including the recurrence-free survival (RFS) and OS, of ARMM patients based on their immune cell infiltration status to search immune-related prognostic biomarkers. Furthermore, we performed gene expression analysis of recurrent and nonrecurrent groups using the NanoString Cancer Immune code set to identify immune pathways and immune cell-type scores associated with the groups.

Materials and methods

Case selection

A total of 22 ARMM cases in the pathology database that had been treated at one hospital from January 2004 to December 2018 were included in the current tertiary single-center study. ARMM was pathologically confirmed after surgical resection in each of these subjects, tissue samples from whom were formalin fixed and paraffin embedded (FFPE). The ARMMs in our present cohort were categorized as anal, rectal, and anorectal, as previously described [23, 24]. Briefly, tumors were defined as anal if lesions were distal to the dentate line, rectal if they were proximal to the dentate line, and anorectal if they arose from the dentate line. Hematoxylin and eosin (H&E)-stained slides of the primary tumors were examined by two expert gastrointestinal pathologists (S-WK and S-MH) to confirm the histological tumor diagnosis and select the appropriate representative slides for subsequent analyses.

Tumor size was obtained from the surgical pathology reports. The following histopathological parameters of the primary ARMM were recorded as previously reported [25]. Tumor thickness was measured from the top of the granular layer of the squamous epithelium or columnar epithelium of the colonic mucosa or from the base of the ulcer to the deepest point of invasion and was categorized according to the T-category criteria (T1, ≤ 1.0 mm; T2, 1.1–2.0 mm; T3, 2.1–4.0 mm; T4, >4.0 mm) of the 8th edition scheme of the American Joint Commission on Cancer (AJCC) cancer staging manual [26]; level of rectal wall invasion (lamina propria, submucosa, muscularis propria, perirectal soft tissue, or serosa and beyond); vertical growth phase [27]; radial growth phase; mitotic

rate [28], determined using the hot spot approach (highest number of mitotic figures in the invasive component/mm²) [29]; tumor-associated epithelial ulceration [30]; lymphovascular invasion [31]; perineural invasion [32]; TILs (Clark's model; absent, non-brisk, or brisk) [33]; immune infiltration phenotype (immune desert, immune excluded, or inflamed); predominant cell type (epithelioid, spindled, or mixed); and final resection margin status were determined after completion of all local surgical procedures (negative, or involved by invasive melanoma).

The stage of disease in each subject was determined based on the 8th edition of the AJCC staging system of cancers of the colon and rectum, cutaneous melanoma, and Ballantyne staging system [34, 35]. A modified Ballantyne staging system was used [36] to assign clinical stage at presentation, as previously reported [25]. The patients were grouped as follows: group L (patients with localized disease confined to the anorectum); group R (patients with regional lymph node metastases); and group D (patients with distant metastases). Data were collected for analysis from the ARMM cases with adequate tissue samples of the primary tumor and available information on recurrences. Recurrence was defined as progressive soft tissue growth or hypermetabolic lesions identified by computed tomography or positron emission tomography with or without biopsy confirmation during follow-up after surgical resection of the ARMM. Clinical data, including patient demographics, treatments (type of operation and adjuvant therapy), recurrences, and survival outcomes, were collected and reviewed from electronic medical records. This study was approved by our Institutional Review Board (approval number: 2017-0955), which waived the requirement for informed consent from the patients due to the retrospective nature of the analyses and the associated minimal risk.

RNA isolation

Representative ARMM and matched normal rectal and/or anal FFPE tissue blocks were selected after a slide review. Cases were carefully manually dissected, and areas containing more than 40% tumor cells were included for total RNA isolation from 5 to 10 FFPE sections with 4 μm thickness. Before transferring the tissues to extraction tubes, non-tumor elements were carefully removed via manual microdissection. After the selected tissue samples were deparaffinized with xylene, total RNA was extracted using an RNeasy FFPE Kit (Qiagen, Hilden, Germany), in accordance with the manufacturer's protocol. RNA was quantified using a NanoDrop2000 spectrophotometer (Thermo Fisher Scientific, DE), and the quality of the RNA was estimated using a 2100 Bioanalyzer (Agilent Technologies, Santa Clara, CA; Supplementary Fig. 1).

NanoString quantification and differential expression

NanoString nCounter nSolver 4.0 software (NanoString, Seattle, WA; MAN-C0019-08), with an additional NanoString Advanced Analysis Module 2.0 plugin (NanoString, MAN-10030-03), was used to perform normalization, differential expression analysis, quality control, and pathway analyses, such as pathway scoring and gene set enrichment analysis. The Advanced Analysis modules use open-source R programming language to perform quality assessment and normalization.

A total of 14 ARMM tissue samples, including 7 recurrent and 7 nonrecurrent melanoma tissue samples, were selected and processed using the Cancer Immune code set on the NanoString nCounter analysis system (NanoString Technologies). Each reaction contained 250 ng of total RNA in a 5 μL aliquot, including capture and reporter probes along with six pairs of positive control probes and eight pairs of negative control probes. Reporter code count (RCC) files and reporter library files (RLF; files specific to cancer immune code set version 1.1) were uploaded into nSolver software, version 4.0 (NanoString, MAN-C0019-08). The NanoString data quality was assessed by default parameters according to the NanoString Gene Expression Data Analysis Guidelines (NanoString, MAN-C0011-04). No background subtraction or background threshold parameters were selected. The geometric mean was used to compute the normalization factors for the mRNA content of 6 positive controls and 40 housekeeping genes. In the fold-change estimation settings, the ratio building option was selected, and the samples were partitioned based on their respective conditions (recurrent vs nonrecurrent). Upon execution, QC flag or normalization flag was identified in the data, indicating good quality.

The geNorm algorithm was implemented, using the 35 most stable housekeeping genes (Supplementary Table 1). Normalized mRNA counts were generated according to the gene expression normalization factor based on the geometric mean of the selected housekeeping genes. For the differential expression module, we applied the optimal statistical method, which comprises: (1) a mixture negative binomial model, (2) a simplified negative binomial model, and (3) a log-linear model for each gene. *P* value adjustments were performed using the Benjamini–Yekutieli method.

Pathway analysis and cell-type profiling

Gene set analysis (GSA) calculates a global differential significance score for each gene set by using the square root of the mean squared *t*-statistic for each to infer the functional roles and measure over- or under-expressed genes in a

pathway (Supplementary Table 2). The PathView module visualizes the top 20 Kyoto Encyclopedia of Genes and Genomes (KEGG) pathways with overlapping significant genes ($P < 0.05$) and selects them on the basis of their fold-change value. A pathway scoring module was used to derive pathway scores using the first principal component of the pathway genes' normalized expression. Plots of pathway scores were selected to be generated against the condition (recurrent vs nonrecurrent). In cell-type profiling, the cell-type abundance was measured by the average log-scale expression of the genes to identify marker genes. Default custom options were selected with dynamic selection of a subset for signature creation and for visualization of all cell types. Raw and relative cell-type abundance was selected with default cell-type contrasts to find in depth patterns in the TIL landscape.

Immunohistochemical staining

Immunohistochemical (IHC) staining was performed using whole sectioned slides to analyze the localization and pattern of the infiltration of immune cells for a total of 22 patients, and NanoString analysis was performed for 14 of these cases. IHC staining was performed using 4- μ m-thick sections prepared from whole section blocks using a BenchMark XT auto immunostainer (Ventana Medical Systems, Oro Valley, AZ), in accordance with the manufacturer's instructions. An alkaline phosphatase kit was used to prevent overestimations due to abundant melanin deposits. Each section was probed with an IHC panel designed to highlight tumor cells expressing PD-L1 (1:100, E1L3N, Cell signaling Technology, Danvers, MA) and other cell types in the infiltrate, including CD3 (1:400, A0452, Dako, Carpinteria, CA), CD8 (1:400, M7103, Dako), Foxp3 (1:100, ab20034, Abcam, Cambridge, UK), CD68 (1:2000, KP-1, Dako), and CD163 (1:400, MOMO, Cell marque, Rocklin, CA). A minimum of 100 viable tumor cells needed to be included in the PD-L1 stained slide for it to be considered adequate for evaluation [37]. Placenta and tonsil tissues were used as an external positive control, whereas macrophages were used as an internal positive control. The results of staining were reviewed independently by two pathologists (S-WK and S-MH) who were blind to the demographic and clinical data. In cases where there were discrepancies in data interpretation, a consensus was reached through a discussion between the two experts.

Quantification of tumor infiltrating lymphocytes

To evaluate the immune contexture, TILs including CD3-, CD8-, and Foxp3-positive T cells, and tumor-associated macrophages (TAMs), including CD68- and CD163-positive cells, were assessed on IHC stained whole sectioned slides.

Two pathologists (S-WK and S-MH) reviewed the H&E slides and carefully selected the most representative areas. The tumor center (TC) and invasion front (IF) of the ARMM lesions were separately evaluated. The IF was defined as the most progressed cancer cells on the advanced edge of the tumor. The hotspots in the TC and IF were selected at low magnification and individually marked on H&E slides and were transferred on IHC stained whole sectioned slides. Four to 10 high power fields (HPF; $\times 400$) in hotspots from each TC and IF were selected. Intratumoral and stromal TILs and TAMs were separately and manually counted from 8 to 20 HPFs in each case. The mean number of TILs and TAMs from HPFs were calculated and used as representative values for further analyses. Intratumoral TILs were defined as lymphocytes in tumor nests having cell-to-cell contact without intervening stroma and directly interacting with melanoma cells, while stromal TILs were dispersed in the stroma between the melanoma cells without direct contact with melanoma cells. TILs or TAMs in tumor areas with crush artifacts, necrosis, or regressive hyalinization were not evaluated [1, 2]. Each TIL type [intratumoral CD3+ (CD3i), stromal CD3+ (CD3s), both intratumoral and stromal CD3+ (CD3), intratumoral CD8+ (cytotoxic T cell, CD8i), stromal CD8+ (CD8s), both intratumoral and stromal CD8+ (CD8), intratumoral Foxp3+ (regulatory T cell (Treg), Foxp3i), stromal Foxp3+ (Foxp3s), both intratumoral and stromal Foxp3+ (Foxp3) T cell, intratumoral CD68+ (CD68i), stromal CD68+ (CD68s), both intratumoral and stromal CD68+ (CD68), intratumoral CD163+ (CD163i), stromal CD163+ (CD163s), both intratumoral and stromal CD163+ (CD163) macrophage] was counted manually at a HPF in the IF and TC. For example, CD3 were counted and presented as CD3i TC; CD3s TC; CD3TC; CD3i IF; CD3s IF; CD3 IF; CD3 Total. The ratio of absolute number of Foxp3 and CD8 in each localization was calculated. Foxp3+Treg cells suppress the induction of cytotoxic CD8+ T lymphocytes in response to cancer cells. Therefore, Foxp3:CD8+T cell ratio may be a sensitive indicator for monitoring immune function in a tumor [21–27]. The Foxp3+/CD8+ ratio was calculated for each specimen using the number in each field (TC, IF, intratumoral, stromal), and the averages were compared.

The determination of cutoff values of each immune cell was evaluated based on the association between OS of the patients and immune contexture score in ARMM data set using the 'maxstat' R survminer package. The R package MaxStat [38–49], which iteratively tests all possible cutoff points to find the one achieving the maximum rank statistic, was used to dichotomize immune contexture score, and patients were then grouped into low and high immune contexture score. Cutoff values were obtained as follows: CD3+ T cells > 20/HPF for CD3 high, CD8+ T cells > 45/HPF for CD8 high, Foxp3+ T cells > 3/HPF for Foxp3 high, Foxp3/CD8 ratio ≥ 10 for Foxp3/CD8 high, CD68+

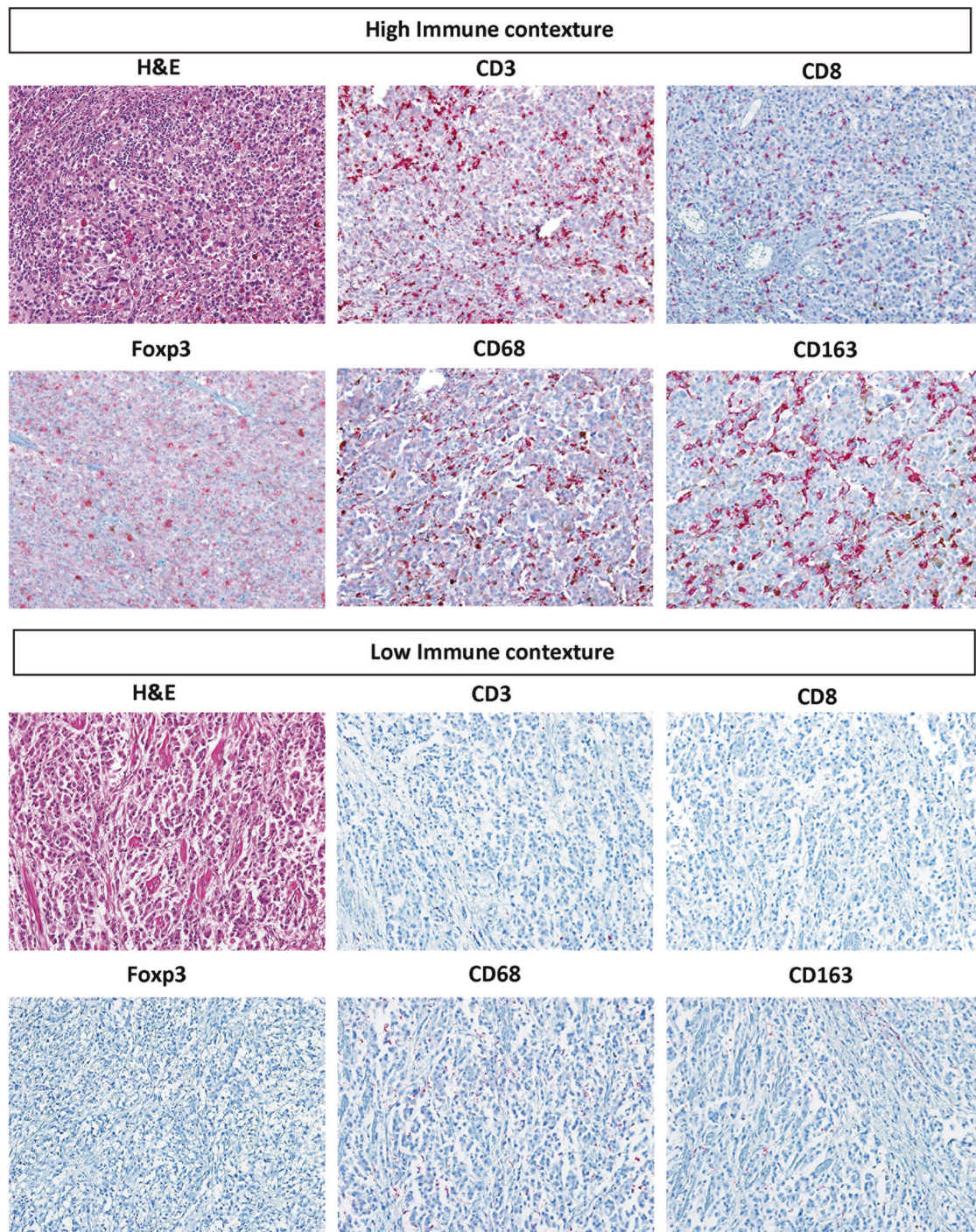


Fig. 1 Representative images of hematoxylin and eosin (H&E) and immunohistochemical staining of the tumor-immune contexture between nonrecurrent (high immune contexture) and recurrent

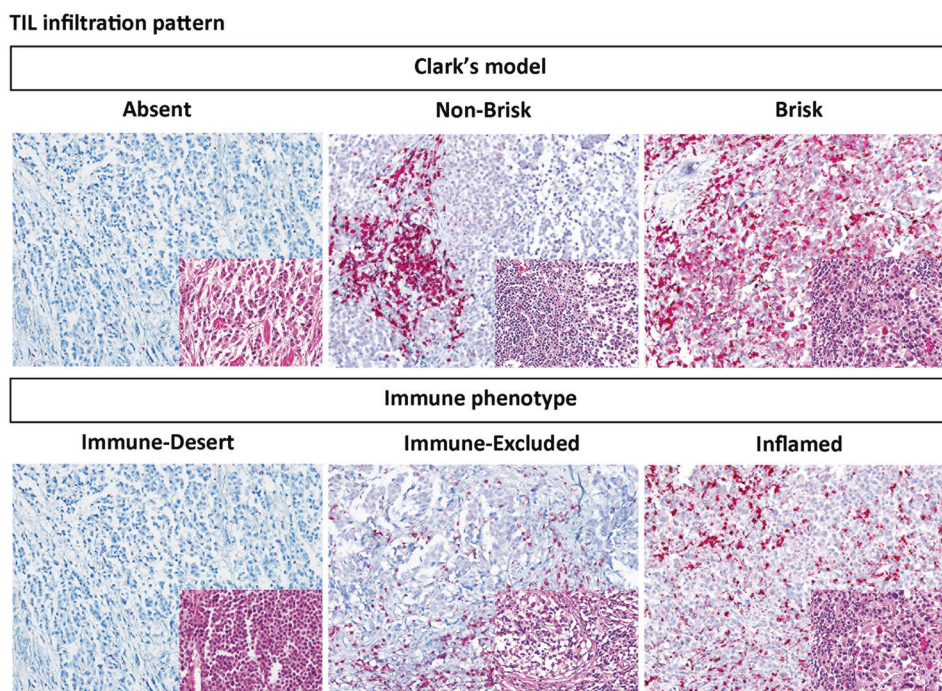
(low immune contexture) patients with anorectal malignant melanoma (ARMM). Original magnification, $\times 200$. Red chromogen indicates each type of immune cells.

macrophages > 10 for CD68 high, CD163+ macrophages > 71 /HPF for CD163 high, and CD163/CD68 ratio ≥ 2.7 for CD163/CD68 high. Figure 1 illustrates the representative H&E staining and immunolabeling patterns for CD3, CD8, Foxp3, CD68, and CD163 from whole sectioned slides in the ARMM cases. All slides were counted manually by two

experts (S-WK and S-MH), who were blinded for clinicopathological data. The two individual scores were compared, and differences in counts of over 10% were reanalyzed until a consensus was reached [2].

PD-L1 expression was evaluated for tumor cells in the TC and IF as previously described [37]. The tumor positive

Fig. 2 Representative H&E and immunohistochemical staining patterns of immune cell infiltration in anorectal malignant melanoma (ARMM). (Upper column) Absent, non-brisk, and brisk CD3+ T lymphocytic infiltration in ARMM. (Lower column) Immune phenotypes in ARMM. Representative images of CD3 immunohistochemistry showing three patterns of T cells associated with malignant melanoma cells. (Lower left) immune-desert, (Lower middle) immune-excluded, and (Lower right) inflamed phenotype. CD3-positive T cell staining is indicated by the red chromogen. The blue color is the hematoxylin counterstain. Original magnification, $\times 200$ (Inset, H&E).



score was counted as the percentage of tumor cells with partial or complete membranous staining of any intensity. Positive immune cells in areas of necrosis were excluded.

TIL infiltration patterns

Adherence to the TIL scoring system described by Clark was followed [50]. Briefly, Clark's model defined the degree of TILs by both the extent and density of the TIL infiltrate: absent, non-brisk (focal TIL infiltrate within the tumor that may be isolated, segmental, or multifocal), and brisk (either diffuse infiltration of the tumor by TILs or a TIL infiltrate across the entire base of the tumor). In addition, in accordance with the TIL quantification and topography, a paradigm for the classification of tumor-immune phenotypes has emerged and three classes of tumors were applied as mentioned in the previous report: i.e. 'immune-desert' tumors (or 'cold' tumors, showing no immune cell infiltration), 'immune-excluded' tumors (with immune cells aggregating at the tumor boundaries) and 'inflamed' tumors (or 'hot' tumors, showing pronounced immune infiltrates in the tumor core (Fig. 2) [51, 52].

Statistical analyses

Statistical analyses were performed using R and Python and two-sided Mann–Whitney *U*-tests and Chi-squared tests were conducted. A Spearman correlation coefficient was used to investigate correlation between two scale variables. Spearman rank-order correlations were measured over every

pair of immune contexture-related variables and death- and recurrence-related variables to understand the monotonicity degree of the pair using Python packages. The Spearman correlation did not assume that both the variables of a pair were normally distributed and varied between -1 and $+1$ with 0 standing for no correlation and between -0.5 and -1 for a strong correlation. For multivariable analysis, we employed logistic regression for present patient data with the scikit-learn_v0.22, Python package. Concordances of counting TILs between two experts were evaluated using the Cohen Kappa statistic. Time to event analysis was performed with two outcomes, OS and RFS. OS was defined from the date of ARMM diagnosis in surviving patients. RFS was defined as the period from the start of treatment and recurrence. The Kaplan–Meier method was used to plot the OS and RFS curves and a log-rank test was used to analyze the significance of differences in survival rates. The Cox regression model was used to analyze the survival impact of continuous variables and to perform multivariable analysis. *P* values < 0.05 were considered to indicate statistical significance.

Results

Clinicopathologic characteristics of the ARMM study cases

Twenty-two patients were analyzed; the detailed characteristics of the patients are summarized in Table 1.

Table 1 Demographic, clinical, and histological characteristics of the 22 ARMM patients.

Parameters	No (%)
Demographics	
Age, years, mean \pm standard deviation	60 \pm 10.8
Sex	
Female	13 (59)
Male	9 (41)
Anatomic site	
Anus	8 (36)
Anorectal junction	6 (28)
Rectum	8 (36)
Operation	
Abdominoperineal resection	19 (86)
Local excision	3 (14)
Tumor size, cm, mean \pm standard deviation	4.9 \pm 2.9
Tumor thickness, mm, mean \pm standard deviation	22 \pm 5.6
Gross	
Ulceration	
Not identified	6 (27)
Present	16 (73)
Growth pattern	
Polypoid/Exophytic	16 (73)
Ulcerofungating	4 (18)
Infiltrative	2 (9)
Pigmentation	
Present	16 (73)
Absent (Amelanotic)	6 (27)
Microscopy	
Predominant cell type	
Epithelioid	7 (32)
Spindled	12 (54)
Mixed	3 (14)
Mitotic count, mean /mm ² [range]	15 (1–59)
In situ component	
Absent	16 (73)
Present	6 (27)
Lymphovascular invasion	
Perineural invasion	7 (32)
Vertical growth phase	
Not identified	1 (5)
Present	21 (95)
Unknown	0 (0)
Radial growth phase	
Not identified	12 (56)
Present	8 (36)
Unknown	4 (18)
Infiltration pattern of immune cells	
Tumor infiltrating lymphocytes	
Absent	7 (32)
Non-brisk	8 (36)
Brisk	7 (32)
Immune phenotype	
Desert	11 (50)
Excluded	5 (23)
Inflamed	6 (27)

Table 1 (continued)

Parameters	No (%)
Stage	
Level of rectal wall invasion	
Lamina propria	0 (0)
Submucosa	5 (23)
Muscularis propria	8 (36)
Perirectal/perianal soft tissue	8 (36)
Serosa and beyond	1 (5)
Pathologic stage (AJCC 8th, cutaneous melanoma)	
pT classification	
1 (\leq 1.0 mm)	0 (0)
2 (1.1–2.0 mm)	0 (0)
3 (2.1–4.0 mm)	0 (0)
without ulceration	0 (0)
with ulceration	1 (5)
4 ($>$ 4.0 mm)	6 (27)
without ulceration	6 (27)
with ulceration	15 (68)
pN classification	
0	9 (41)
1	7 (32)
2	3 (14)
3	3 (14)
Stage	
I	0 (0)
II	8 (36)
III	8 (36)
IV	6 (28)
Ballantyne staging system	
I	5 (24)
II	8 (36)
III	6 (28)
Clinical stage at presentation (modified Ballantyne staging system)	
Localized disease (Group L)	8 (36)
Regional metastases (Group R)	8 (36)
Distant metastases (Group D)	6 (28)
Treatment and outcome	
Involvement of radial margin	3 (14)
Adjuvant therapy	
Radiotherapy	5 (23)
Chemotherapy	3 (14)
Immunotherapy	2 (9)

ARMM Anorectal malignant melanoma, AJCC American Joint Committee on Cancer.

Briefly, mean patient ages was 60.0 years [standard deviation (SD), 10.8 years]. The male: female ratio was 0.7. The tumor was located in the anus in eight cases (36%), at the anorectal junction in six cases (28%), and in the rectum in eight cases (36%). Nineteen (86%) of the patients were treated with abdominoperineal resection and three (14%) underwent a local excision. The mean tumor size was 4.9 cm (SD, \pm 2.9 cm). Tumor thickness was $>$ 4.0 mm in 21 cases (96%), with a mean of 22 mm; 16 (73%) tumors were

ulcerated. Polypoid/exophytic was the most common growth pattern (16 cases, 73%). Sixteen cases (73%) had melanin pigments ranging from local pigment cluster to diffusely distributed. However, melanin pigment was not observed in the remaining six patients (27%, amelanotic). The predominant cell types were epithelioid (7 cases, 32%), spindled (12 cases, 54%), and mixed (3 cases, 14%). The mean mitotic rate was 15/mm². Melanoma in situ component within squamous mucosa was in six cases (27%). Lymphovascular and perineal invasion were present in seven (32%) and two (9%) patients, respectively. Extension into the muscularis propria and perirectal/perianal soft tissue was the most frequent and was identified in 16 patients (72%). Most cases were pT4 (21 cases, 95%) (cutaneous melanoma staging). Regional nodal and distant metastasis at the time of diagnosis occurred in 13 (60%) and 6 cases (28%), respectively. Eight cases (36%) had disease confined to the anorectum. A variety of approaches to systemic therapy were employed in the neoadjuvant and adjuvant settings. The median follow-up period was 25.5 months (interquartile range (IQR), 10.8–58.0). As an adjuvant treatment, five patients received radiotherapy, two patients received chemotherapy with combination of dacarbazine, BCNU (carmustine), cisplatin, and tamoxifen. One patient received chemotherapy with a combination of dacarbazine, cisplatin, and vinblastine sulfate, and two patients received interferon alfa-2a. The recurrence rate was 50%, with 11 patients experiencing disease recurrence over a median disease-free interval of 6 months (IQR, 3–10). Most were distant recurrences (8 cases, 73%), with the most common recurrent site occurring in the liver (5 cases, 45%). Ten patients died with disease and two patients of other causes.

Gene expression analysis

We originally performed gene expression analysis in all 22 cases, of which 8 cases had poor RNA quality and were excluded from gene expression analysis. Finally, differential gene expression analysis was conducted for 14 samples, including 7 recurrent and 7 nonrecurrent ARMM samples. Supplementary Fig. 2A shows the supervised hierarchical clustering and emphasizes the differences between the recurrent and nonrecurrent ARMMs. Differential gene expression analysis results identified 229 downregulated and 1 up regulated gene between the recurrent and nonrecurrent groups ($P < 0.05$ and a log-fold change $> |1.5|$; Supplementary Fig. 2B).

Pathway score analysis was performed for the differentially expressed genes to compare the relative pathway score differences between the recurrent and nonrecurrent ARMM groups. The results revealed significantly decreased pathway scores in the recurrent samples, such as those involved

in regulation, chemokines, and cell function, as opposed to the increased gene expression in these pathways in the nonrecurrent samples (Supplementary Fig. 3A). Out of 22 pathways evaluated in this analysis, 15 pathways related to the immune system exhibited a downregulation (low pathway scores) in the recurrent group (Supplementary Fig. 3A).

Cell-type profiling results indicated the TIL scores for the T-cell, B-cell, and macrophage profiles. The recurrent group had a significantly lower TIL score in T-cell and B-cell profiles (all, $P < 0.01$) and lower macrophage score ($P = 0.05$) than nonrecurrent group (Supplementary Fig. 3B).

A high TIL is significantly associated with a favorable prognosis in ARMM

To address whether immune cell infiltration is associated with the prognosis in patients with ARMM, we quantified the immune cell infiltration in tumor tissue with IHC staining and manually counted them. Comparison of immune contexture based on the localization of immune cells and recurrence and survival outcome are summarized in Table 2 and Fig. 3a. Overall, the density of immune cells in the recurred group was significantly lower or tended to be lower than that in the nonrecurrent group, which was consistent with the results of RNA analysis. In particular, in all analyzed TIL subtypes, the recurrent group had a significantly lower number of infiltrating immune cells in the intratumoral area in the TC than the nonrecurrent group [mean \pm SD (range): CD3, 40 \pm 40.8 (2–118) vs 95 \pm 79.7 (5–195), $P = 0.005$; CD8, 13 \pm 12.0 (1–39) vs 22 \pm 51.6 (1–155), $P < 0.001$; Foxp3, 3 \pm 11.7 (0–36) vs 10 \pm 21.9 (0–64), $P = 0.027$]. In addition, in the recurrent group, regardless of the location of immune cell infiltration, whether it be the TC or IF, infiltration of CD3+ T cells in both the intratumoral and stromal areas was significantly lower than in the nonrecurrent group (CD3; TC, 71 \pm 83.6 (14–246) vs 207 \pm 165.6 (9–420), $P = 0.004$, IF, 169 \pm 70.2 (35–285) vs 301 \pm 157.4 (29–502), $P = 0.021$). Subsequently, the density of total CD3+ and CD8+ TILs (TC + IF) was significantly lower in the recurrent group [CD3, 234 \pm 129 (100–531) vs 576 \pm 268 (41–876), $P = 0.022$; CD8, 102 \pm 60 (53–246) vs 207 \pm 159 (59–482), $P = 0.007$]. The density of macrophage infiltration between the recurrent and nonrecurrent group was significantly different in the IF [CD68, intratumoral, 20 \pm 27.3 (6–55) vs 38 \pm 27.0 (10–175), $P = 0.016$; CD163, intratumoral, 30 \pm 21.0 (6–82) vs 49 \pm 36.1 (16–117), $P = 0.028$, stromal, 16 \pm 14.3 (5–50) vs 23 \pm 28.5 (3–80), $P = 0.03$]. The total TILs (sum of total CD3-, CD8- and Foxp3-positive cells) were more abundant in the nonrecurrent and surviving group than in the recurrent and deceased group regardless of location [351 \pm 185 (185–689) vs 751 \pm 485 (135–1524), $P = 0.049$; 410 \pm 208 (135–793) vs 803 \pm 416 (216–1524), $P = 0.037$], which

Table 2 Comparison of immune contexture considering location according to survival outcome.

Parameters	Recurrent Mean ± SD (range) (N = 11)	Nonrecurrent Mean ± SD (range) (N = 11)	P	Deceased Mean ± SD (range) (N = 12)	Surviving Mean ± SD (range) (N = 10)	P
CD3						
TC						
Intratumoral (i)	40 ± 40.8 (2–118)	95 ± 79.7 (5–195)	0.005*	31 ± 51.4 (2–118)	102 ± 75.8 (4–195)	0.13
Stromal (s)	4 ± 2.0 (1–8)	3 ± 4.8 (0–15)	0.032*	4 ± 2.0 (0–7)	6 ± 4.6 (0–15)	0.024*
Both (i + s)	71 ± 83.6 (14–246)	207 ± 165.6 (9–420)	0.004*	103 ± 103 (12–349)	219 ± 157 (9–420)	0.10
IF						
Intratumoral (i)	32 ± 38.1 (13–134)	35 ± 62.0 (12–218)	0.16	31 ± 43.4 (12–134)	40 ± 60.4 (12–218)	0.58
Stromal (s)	19 ± 24.2 (2–72)	95 ± 83.8 (3–220)	<0.001*	15 ± 39.1 (2–134)	65 ± 84.6 (6–220)	0.007*
Both (i + s)	169 ± 70.2 (35–285)	301 ± 157.4 (29–502)	0.021*	178 ± 93 (29–316)	261 ± 162 (104–502)	0.013*
Total (TC + IF)	234 ± 129 (100–531)	576 ± 268 (41–876)	0.022*	237 ± 171 (41–606)	554 ± 263 (150–876)	0.09
CD8						
TC						
Intratumoral (i)	13 ± 12.0 (1–39)	22 ± 51.6 (1–155)	<0.001*	13 ± 17.4 (7–33)	22 ± 54.2 (1–155)	0.001*
Stromal (s)	1 ± 5.7 (0–20)	1 ± 3.98 (0–12)	0.96	1 ± 5.5 (0–3)	4 ± 4.0 (0–20)	0.94
Both (i + s)	36 ± 25.2 (2–82)	101 ± 107 (2–330)	0.001*	46 ± 34 (12–132)	99 ± 112 (2–330)	0.001*
IF						
Intratumoral (i)	19 ± 9.2 (4–31)	24 ± 33.4 (5–102)	0.010*	16 ± 9.5 (4–31)	22 ± 34.4 (4–102)	0.004*
Stromal (s)	17 ± 21.4 (2–78)	20 ± 18.6 (1–61)	0.98	16 ± 17.4 (11–61)	18 ± 22.8 (4–31)	0.52
Both (i + s)	60 ± 48.9 (30–194)	108 ± 75.7 (12–265)	0.16	57 ± 37 (30–148)	110 ± 81 (12–265)	0.022*
Total (TC + IF)	102 ± 60 (53–246)	207 ± 159 (59–482)	0.007*	110 ± 47 (55–195)	215 ± 169 (53–482)	<0.001*
Foxp3						
TC						
Intratumoral (i)	3 ± 11.7 (0–36)	10 ± 21.9 (0–64)	0.027*	3 ± 5.1 (0–10)	20 ± 12.5 (0–64)	0.001*
Stromal (s)	0 ± 0.3 (0–2)	0.5 ± 1.3 (0–4)	<0.001*	1 ± 0.4 (0–1)	1 ± 0.1 (0–4)	<0.001*
Both (i + s)	16 ± 23.7 (0–73)	41 ± 45.7 (0–135)	0.026*	9 ± 14 (12–132)	51 ± 44 (2–135)	0.001*
IF						
Intratumoral (i)	4 ± 9.1 (1–32)	9 ± 20.0 (1–73)	0.30	4 ± 8.3 (1–15)	8 ± 20.8 (1–73)	0.23
Stromal (s)	1 ± 1.4 (0–4)	1 ± 2.6 (0–6)	0.026*	1 ± 1.3 (0–4)	2 ± 2.6 (0–6)	0.009*
Both (i + s)	9 ± 20.2 (2–70)	20 ± 42.8 (2–157)	0.37	15 ± 19 (2–70)	33 ± 44 (2–157)	0.26
Total (TC + IF)	32 ± 40 (2–121)	73 ± 71 (2–216)	0.06	25 ± 33 (4–216)	85 ± 70 (4–216)	0.015*
Foxp3/CD8 ratio						
TC						
Intratumoral (i)	13.5 ± 12.0 (1–39)	22 ± 51.3 (1–155)	<0.001*	13 ± 17 (5–65)	22 ± 54 (1–155)	0.001*
Stromal (s)	3.5 ± 11.7 (0–36)	10 ± 22.0 (0–64)	0.027*	2 ± 7 (0–25)	20.50 ± 21 (1–64)	0.001*
Both (i + s)	1.75 ± 1.0 (0–18.25)	5 ± 2 (0–33.75)	0.026*	1 ± 1.8 (0.0–12.75)	11.5 ± 10 (0.5–33.75)	0.001*
IF						
Intratumoral (i)	0.28 ± 0.4 (0–1)	0.39 ± 0.7 (0–2)	0.14	0.26 ± 0.6 (0–2)	0.38 ± 0.5 (0–2)	0.25
Stromal (s)	0.1 ± 0.5 (0–2)	0.01 ± 0.3 (0–1)	0.45	0 ± 0.4 (0–2)	0.1 ± 0.2 (0–1)	0.55
Both (i + s)	0.18 ± 0.1 (0.02–1.38)	0.27 ± 0.1 (0.02–1.17)	0.92	0.15 ± 0.5 (0.02–1.38)	0.27 ± 0.3 (0.06–1.17)	0.13
Total (TC + IF)	0.96 ± 0.5 (0.05–9.31)	2.83 ± 1.7 (0.01–17.01)	0.035*	0.72 ± 0.5 (0.01–7.06)	5.95 ± 6.8 (0.28–17.01)	0.001*
CD68						
TC						
Intratumoral (i)	23 ± 15.3 (6–87)	51 ± 52.0 (5–89)	0.94	33 ± 29.8 (9–87)	36 ± 25.4 (5–89)	0.49
Stromal (s)	3 ± 8.0 (1–4)	6 ± 9.1 (1–18)	0.012*	4 ± 2.3 (1–10)	5 ± 4.9 (1–18)	0.07
Both (i + s)	70 ± 55.1 (16–181)	113 ± 55.1 (11–188)	0.97	71 ± 53 (23–188)	94 ± 61 (11–186)	0.41

Table 2 (continued)

Parameters	Recurrent Mean ± SD (range) (<i>N</i> = 11)	Nonrecurrent Mean ± SD (range) (<i>N</i> = 11)	<i>P</i>	Deceased Mean ± SD (range) (<i>N</i> = 12)	Surviving Mean ± SD (range) (<i>N</i> = 10)	<i>P</i>
IF						
Intratumoral (i)	20 ± 27.3 (6–55)	38 ± 27.0 (10–175)	0.016*	23 ± 21 (10–55)	35 ± 55 (6–175)	0.046*
Stromal (s)	5 ± 1.0 (2–23)	10 ± 4.7 (5–36)	0.79	5 ± 10.5 (2–36)	10 ± 5.8 (2–23)	0.14
Both (i + s)	59 ± 28.9 (24–130)	119 ± 103.4 (29–375)	0.019*	77 ± 44 (24–175)	133 ± 110 (40–375)	0.06
Total (TC + IF)	339 ± 211 (147–853)	504 ± 592 (132–1829)	0.008*	351 ± 143 (150–543)	785 ± 623 (132–1829)	0.001*
CD163						
TC						
Intratumoral (i)	55 ± 61.0 (7–207)	91 ± 65.2 (8–229)	0.93	76 ± 58 (7–207)	75 ± 69.7 (15–229)	0.54
Stromal (s)	5 ± 3.2 (4–15)	8 ± 4.1 (4–18)	0.36	5 ± 4.4 (4–18)	7 ± 2.8 (4–13)	0.26
Both (i + s)	120 ± 52 (40–429)	198 ± 31 (51–467)	0.90	162 ± 52 (40–429)	162 ± 64 (47–462)	0.46
IF						
Intratumoral (i)	30 ± 21.0 (6–82)	49 ± 36.1 (16–117)	0.028*	24 ± 21.5 (6–46)	32 ± 36.8 (16–116)	0.013*
Stromal (s)	16 ± 14.3 (5–50)	23 ± 28.5 (3–80)	0.03*	13 ± 21.5 (3–73)	7 ± 24.8 (4–80)	0.83
Both (i + s)	89 ± 35.8 (41–176)	162 ± 79.1 (45–253)	0.005*	91 ± 47 (41–181)	121 ± 83 (48–253)	0.004*
Total (TC + IF)	1171 ± 723 (463–2838)	2402 ± 1935 (406–5978)	0.009*	1086 ± 481 (463–1820)	2578 ± 2026 (406–5978)	0.001*
Total						
Total TIL (CD3 + CD8 + Foxp3)						
TC	113 ± 114.2 (23–361)	375 ± 279.6 (13–885)	0.007*	110 ± 134 (31–481)	368 ± 278 (13–885)	0.001*
IF	238 ± 85.4 (87–350)	460 ± 245.6 (104–886)	0.003*	254 ± 116 (89–495)	394 ± 245 (182–886)	0.007*
TC + IF	351 ± 185 (185–689)	751 ± 485 (135–1524)	0.049*	410 ± 208 (135–793)	803 ± 416 (216–1524)	0.037*
Total TAM (CD68 + CD163)						
TC	223 ± 164 (63–587)	315 ± 160 (75–591)	0.96	269 ± 160 (68–587)	266 ± 178 (63–591)	0.63
IF	142 ± 50.9 (103–267)	300 ± 137.9 (74–588)	0.07	180 ± 82 (74–332)	272 ± 148 (105–588)	0.14
TC + IF	1535 ± 934 (613–3691)	3139 ± 2527 (536–7807)	0.009*	1437 ± 624 (613–2329)	3363 ± 2649 (538–7807)	0.001*

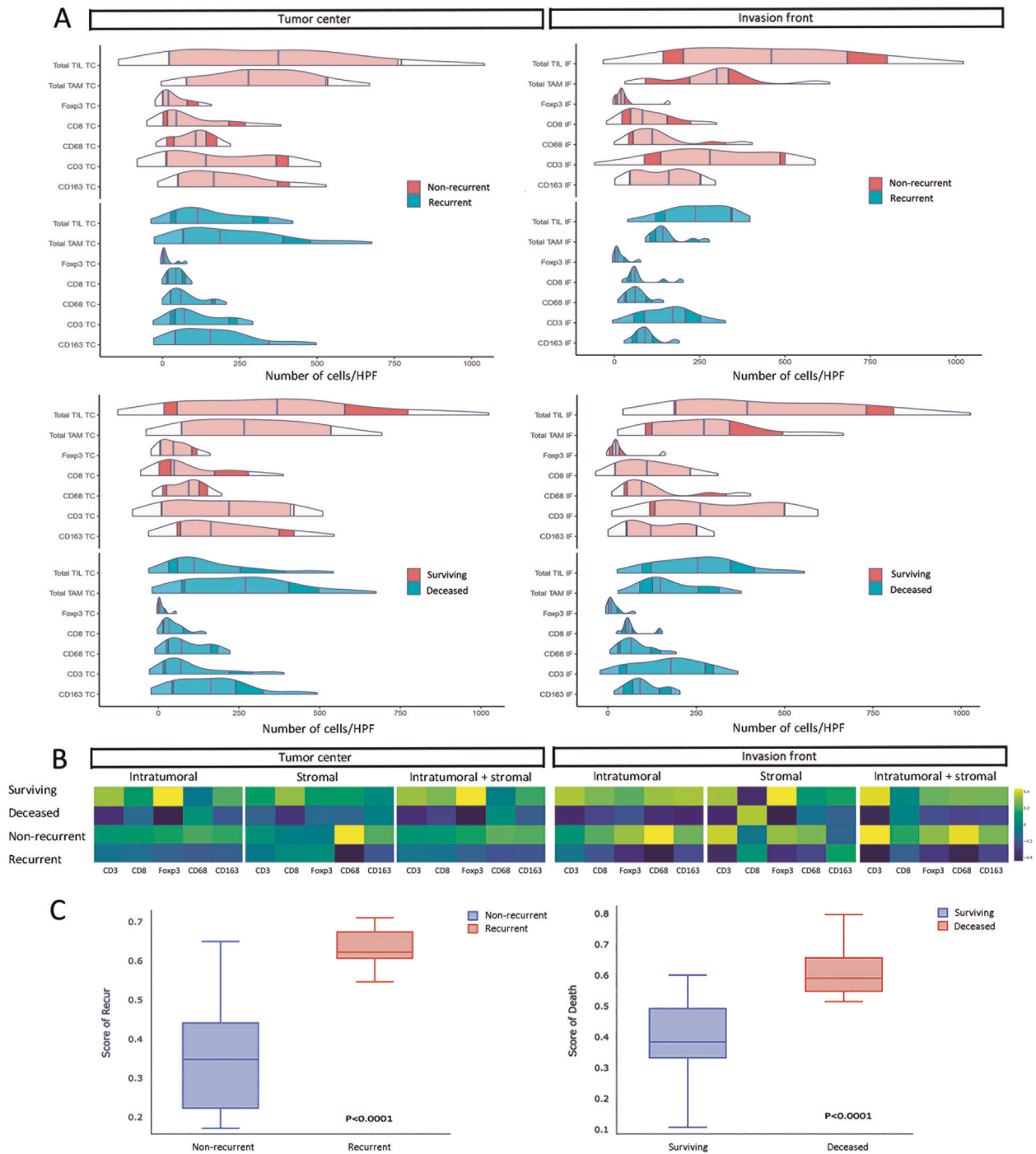
TIL tumor infiltrating lymphocytes, *TAM* tumor-associated macrophage, *TC* tumor center, *IF* Invasion front, *SD* standard deviation.

*Significant *P* < 0.05.

was corroborated with RNA analysis. When the deceased and surviving groups were compared, the results were similar to those stated above (Table 2). In summary, immune cell infiltration was significantly different between the non-recurrent and/or surviving group and the recurrent and/or deceased group, and in particular, a significant difference in the infiltration of intratumoral tumor cells at the TC was observed in two different prognostic groups. The recurrent group had significantly lower total Foxp3 IFs compared to the nonrecurrent group (Supplementary Table 3, *P* = 0.027). Similarly, the deceased group had a significantly lower CD3+ T cell in the IF compared to the surviving group (Supplementary Table 3, *P* = 0.036) after dichotomization based on cutoff value. No significant survival difference was observed between recurrent/deceased and nonrecurrent/surviving groups (*P* = 0.65 and 0.62, respectively) based on PD-L1 labeling (Supplementary Table 3).

Scoring of recurrence and death

We analyzed the association between the immune contexture and survival outcome. Every pair of immune contextures-related variables is visualized in the heatmap as illustrated in Fig. 3b. Figure 3 shows that strongly negative correlations were evident in pairs of death and CD3i, Foxp3i, Foxp3, and CD8s in the TC and CD3i, CD68i, CD163i, CD3s, Foxp3s, and CD3 at the IF. Furthermore, strongly negative correlations were also evident in pairs of recurrence and CD68s in the TC, and Foxp3i, CD68i, CD3s, Foxp3s, CD68s, CD3, and CD68 at the IF. In multivariable analysis, duplicated columns were first averaged, and all data were normalized in a column-wise fashion between 0 and 1 using MinMax Scaler of scikit learn to avoid issues with a learning model being too sensitive to particular columns. We then defined two dependent



variables for two different models, recurrence prediction model (RPM) and death prediction model (DPM), as 1 for recurrence and 0 for non-recurrence in the RPM and 1 for death and 0 for survival in the DPM. By logistic regression with the default setting, we obtained an RPM area under the curve (AUC) of 0.92 and DPM AUC of 0.95. The coefficient tables of these two models are shown in Supplementary Table 4 and indicated the mutual influence degree, in

association with other variables, of every variable with a 0 standing for no influence and a higher absolute value for more influence. These score distributions are presented in Fig. 3c. The Mann–Whitney *U* statistical analysis of the scores between recurrence and non-recurrence resulted in a *P* value of <0.0001 and of those between death and survival in a *P* value of <0.0001. This indicated that both models successfully differentiated the two groups of interest.

◀ Fig. 3 Correlation of immune contexture and survival using immunohistochemistry. **a** Comparison of infiltration density of tumor infiltrating lymphocytes (TILs) according to the survival outcomes in the anorectal malignant melanoma (ARMM) patients. The density of the total TILs (sum of CD3-, CD8-, and Foxp3-positive cells), CD3-, and Foxp3-positive T cells are significantly higher abundant in the surviving group. **b** Correlation of immune contexture-related variables (CD3, CD8, Foxp3, CD68, and CD163) and outcomes (surviving, deceased, nonrecurrent, recurrent) of the patients with ARMM. Dark navy and yellow indicates negative and positive correlation, respectively. Strong negative correlations are shown in the pairs of deceased patients and intratumoral CD3+ (CD3i), Foxp3+ (Foxp3i), stromal CD8+ (CD8s) and both intratumoral and stromal Foxp3+ (Foxp3) T cells in tumor center (TC) (Left panels). Similarly, strong negative correlations are shown in the pairs of deceased patients and CD3i, intratumoral CD68+ (CD68i), CD163+ (CD163i), stromal CD3+ (CD3s), Foxp3+ (Foxp3s), and both CD3+ (CD3) T cells in invasion front (IF). Furthermore, strongly negative correlations (dark navy) are also shown in pairs of recurrent patients and stromal CD68+ (CD68s) macrophage in TC, and Foxp3i, CD68i, CD3s, Foxp3s, CD68s, both intratumoral and stromal CD3+ (CD3) T cells and CD68+ (CD68) macrophage in IF. **c** Comparison of recurrent/deceased ARMM patient group and nonrecurrent/surviving group using recurrence prediction model (RPM) and death prediction model (DPM). Mann-Whitney *U* statistics for the nonrecurrent and recurrent groups yielded a *P* value of <0.0001 and that between the alive and dead groups a *P* value of <0.0001.

A low TIL was associated with poor overall survival in anorectal malignant melanoma

The median OS (17 months) of the recurrence group was significantly shorter than that of the nonrecurrent group (82 months, $P = 0.003$). In patients with ARMM having higher immune cell infiltration, the OS and RFS were significantly improved or tended to be better (Fig. 4 and Supplementary Figs. 4–9). More specifically, when patients with ARMM had high intratumoral CD3+ T cells at the IF (Supplementary Fig. 4A), high intratumoral CD8+ T cells in the TC (Supplementary Fig. 4G), high stromal CD3+ T cells in the TC (Supplementary Fig. 4D), and high stromal Foxp3+ T cells at the IF (Supplementary Fig. 4J), they had significantly better OS than patients with ARMM having low intratumoral CD3+ T cells at the IF, low intratumoral CD8+ T cells in the TC, low stromal CD3+ T cells in the TC, and low stromal Foxp3+ T cells at the IF, respectively (CD3i IF, 1-year survival rate (1YSR), 35.7% vs 87.5%, $P = 0.0013$, [95% confidential interval (95% CI), 0.01–0.46], Supplementary Fig. 4A; CD3s TC, 1YSR, 28.5% vs 66.7%, $P = 0.033$, 95% CI, 0.04–0.79, Supplementary Fig. 4D; CD8iTC, 1YSR, 21.5% vs 71.7%, $P = 0.021$, 95% CI, 0.003–0.25, Supplementary Fig. 4G; Foxp3sIF, 1YSR, 37.5% vs 74.7%, $P = 0.016$, 95% CI, 0.01–0.87, Supplementary Fig. 4J). Similarly, when patients with ARMM had high intratumoral CD3+ (Supplementary Fig. 5A) and high intratumoral CD8+ (Supplementary Fig. 5E) T cells at the IF, and high stromal CD3+ T cells in the TC (Supplementary Fig. 5D), they had significantly

better RFS than those with low intratumoral CD3+ and low intratumoral CD8+ T cells at the IF, and low stromal CD3+ T cells in the TC, respectively (CD3i IF, 1YSR, 22.4% vs 71.6%, $P = 0.002$, 95% CI, 0.004–0.99, Supplementary Fig. 5A; CD3s TC, 1YSR, 42% vs 78.1%, $P = 0.01$, 95% CI, 0.04–1.09, Supplementary Fig. 5D; CD8iIF, 1YSR, 25.1% vs 75.4%, $P = 0.028$, 95% CI, 0.01–0.79, Supplementary Fig. 5E).

ARMM patients with high intratumoral CD68+ in the TC (Supplementary Fig. 6C), and stromal CD163+ macrophages in the TC (Supplementary Fig. 6H) had significantly better OS than those with low intratumoral CD68+, and stromal CD163+ macrophages in the TC (CD68iTC, 1YSR, 35.7% vs 87.5%, $P = 0.036$, 95% CI, 0.11–0.46, Supplementary Fig. 6C; CD163sTC, 1YSR, 0% vs 76.7%, $P < 0.001$, 95% CI, 0.003–0.14, Supplementary Fig. 6H). Similarly, patients with ARMM having high intratumoral CD68+ macrophage in the TC (Supplementary Fig. 7C) and high stromal CD163+ macrophages in the TC (Supplementary Fig. 7H) had significantly better RFS than those with low intratumoral CD68+ macrophage and high stromal CD163+ macrophages in the TC (CD68iTC, 1YSR, 34% vs 91.6%, $P < 0.001$, 95% CI, 0.004–0.46, Supplementary Fig. 7C; CD163sTC, 1YSR, 27.2% vs 71.8%, $P = 0.01$, 95% CI, 0.02–0.55, Supplementary Fig. 7H). Of note, patients with ARMM having high total TIL (sum of T cell subsets, Fig. 4a and Supplementary Fig. 8A) and TAM (Fig. 4b and Supplementary Fig. 8B) had significantly better OS and RFS than those with low total TIL and TAM, respectively (total TIL, 1YSR, 35.7% vs 87.5%, $P = 0.007$, 95% CI, 0.01–0.35, Fig. 4a; total TAM, 1YSR, 28.5% vs 66.7%, $P = 0.035$, 95% CI, 0.02–0.79, Fig. 4b). In addition, patients with ARMM with high-CD3+ T-cell infiltration (both intratumoral and stromal) in the tumor IF (Fig. 4c), and in TC (Fig. 4d), high CD8-positive T cell infiltration in the TC (Fig. 4f) and Foxp3-positive T-cell infiltration in the IF (Fig. 4g) and TC (Fig. 4h) show significantly better OS and RFS than those with low infiltration (CD3 IF, 1YSR, 25.2% vs 82.4%, $P < 0.001$, 95% CI, 0.005–0.23, Fig. 4c; CD3TC, 1YSR, 36.3% vs 72.7%, $P = 0.049$, 95% CI, 0.55–0.88; Fig. 4d; CD8TC, 1YSR, 44.4% vs 81.6%, $P = 0.028$, 95% CI, 0.44–0.99, Fig. 4f; Foxp3IF, 1YSR, 22.2% vs 79.8%, $P = 0.03$, 95% CI, 0.01–0.79, Fig. 4g; Foxp3TC, 1YSR, 27.2% vs 76.8%, $P = 0.008$, 95% CI, 0.01–0.79, Fig. 4h). Similarly, patient with ARMM with high CD68+ and CD163+ macrophages infiltration (both intratumoral and stromal) in IF (Supplementary Fig. 9A, B) show significantly better OS than those with low infiltration (CD68IF, 1YSR, 0% vs 60%, $P = 0.038$, 95% CI, 0.40–1.09, Supplementary Fig. 9A; CD163IF, 1YSR, 28.5% vs 100%, $P = 0.048$, 95% CI, 0.52–1.29, Supplementary Fig. 9B). Considering total Foxp3/CD3 ratio, patient with ARMM with high ratio had significantly better OS than

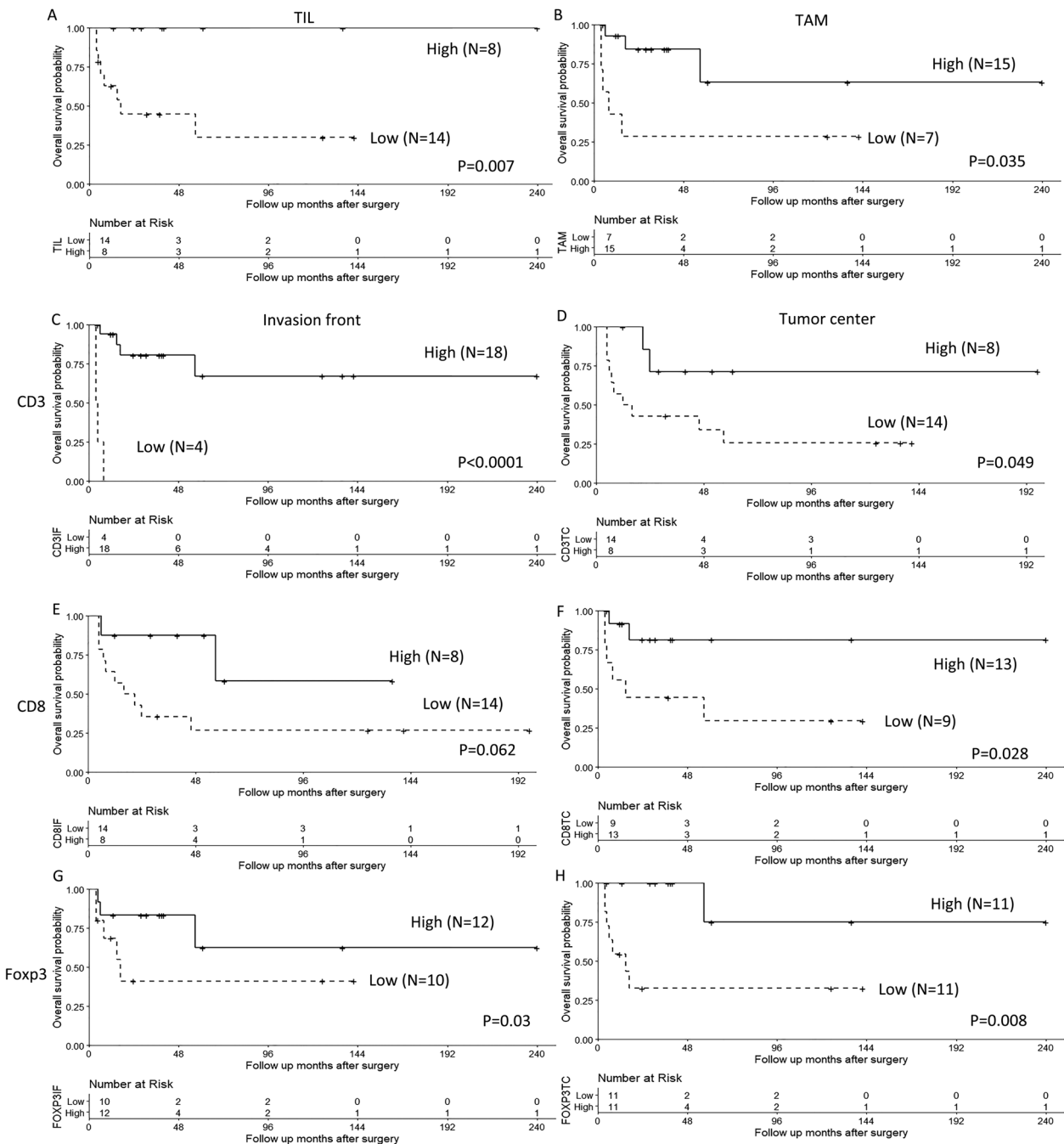


Fig. 4 Kaplan–Meier curves generated in accordance with the immune contexture and immune cell localization in patients with anorectal malignant melanoma (ARMM). a, b Patients with high tumor infiltrating lymphocytes (TIL) and tumor-associated macrophages (TAM) infiltrations show significantly better prognosis than those with low TIL and TAM infiltration ($P = 0.007$ and $P = 0.035$, respectively). **c, d** Patients with ARMM with high CD3+ T-cell infiltration in the tumor invasion front ($P < 0.001$), and in tumor center

($P = 0.049$), **f** high CD8+ T cell infiltration in the tumor center ($P = 0.028$) and **g, h** Foxp3+ T-cell infiltration in the invasion front ($P = 0.033$) and tumor center ($P = 0.0088$) show significantly better overall survival than those with low infiltration. Patients **e** CD8+ T-cell infiltration of the invasion front ($P = 0.062$) have no significant difference in terms of survival, but they show a trend toward a better overall survival compared to the low infiltration.

those with low ratio (1YSR, 20% vs 83.3%, $P < 0.001$, 95% CI, 0.13–0.78, Supplementary Fig. 9C). Among the TIL types, the 1YSR of patients with ARMM having a high number of CD8+ T cells at the IF was not significantly

different compared to those with a low number of CD8+ T cells, but they show a trend toward a better OS and RFS compared to those with low infiltration (Fig. 4e and Supplementary Fig. 8E).

Table 3 Overall survival analyses of the study patients with ARMM ($n = 22$).

Factor	Univariate analysis		<i>P</i>	Multivariate analysis		<i>P</i>
	HR	95% CI		HR	95% CI	
Immune contexture (Both (i + s))						
CD3						
Invasion front	0.124	0.005–0.23	<0.0001*	0.21	0.01–0.41	0.003*
Tumor center	0.336	0.55–0.88	0.049*	0.98	0.35–1.13	0.34
CD8						
Invasion front	0.423	0.11–1.57	0.06			
Tumor center	0.264	0.44–0.99	0.028*	0.78	0.12–3.78	0.14
Foxp3						
Invasion front	0.377	0.017–0.79	0.03*	0.64	0.06–6.24	0.7
Tumor center	0.097	0.012–0.79	0.008*	1.03	0.07–15.78	0.98
CD68						
Invasion front	0.209	0.40–1.09	0.038*	0.227	0.04–1.22	0.08
Tumor center	27.73	0.004–1.75	0.1			
CD163						
Invasion front	0.156	0.52–1.29	0.048*	0.346	0.04–1.92	0.97
Tumor center	0.372	0.09–1.59	0.1			
Stage						
Pathologic stage (AJCC 8th, Cutaneous melanoma)						
pT			0.002*			0.83
3 with ulceration	1			1		
4 without ulceration	0.305	0.03–3.38		0.429	0.04–5.07	
4 with ulceration	1.032	0.08–12.77		1.704	0.12–23.84	
pN			0.024*			0.64
0	1			1		
1	2.726	0.30–24.49		2.25	0.19–27.37	
2	9.33	1.22–71.33		1.458	0.55–38.75	
3	11.899	1.12–118.42		0.795	0.03–21.84	
Clinical stage at presentation			0.68			
Localized disease (Group L)	1					
Regional metastases (Group R)	1.691	0.40–7.12				
Distant metastases (Group D)	1.912	0.43–8.58				

ARMM anorectal malignant melanoma, CI confidence interval, HR hazard ratio.

*Significant $P < 0.05$.

CD3+ TILs at the invasion front act as an independent and positive prognostic indicator in anorectal melanoma

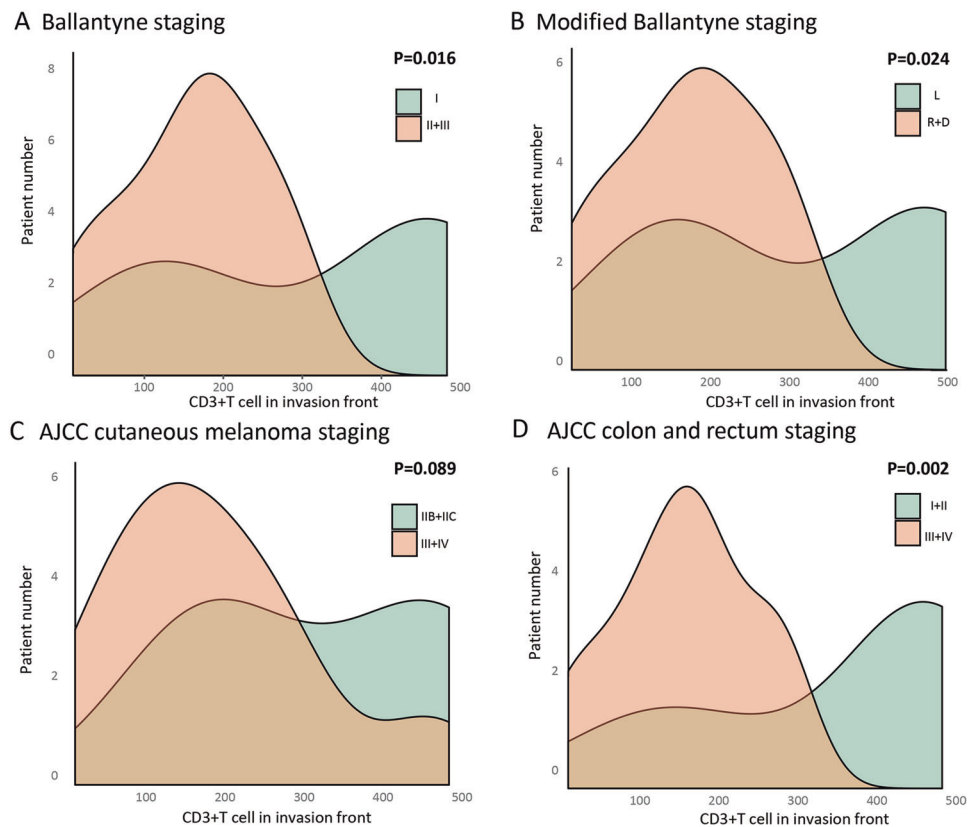
Significant OS improvements were observed in patients with a high CD3 IF (Fig. 4c), CD3TC (Fig. 4d), CD8TC (Fig. 4f), Foxp3IF (Fig. 4g), Foxp3TC (Fig. 4h), CD68IF (Supplementary Fig. 9A), and CD163IF (Supplementary Fig. 9B). To determine whether the density or subtype of TIL was an independent prognostic factor, the Cox regression analysis with other clinicopathologic factors was conducted. Factors showing statistical significance in the univariate analysis were included in the subsequent

multivariate analysis, wherein, after adjusting for these variables, a high CD3 IF was still an independent prognostic factor for OS (Table 3; HR = 0.21, $P = 0.003$, 95% CI = 0.01–0.41).

High-CD3+ T cells in invasion front are significantly associated with low stages in ARMM

Since CD3 IF in ARMM was remained as an independent prognostic factor by multivariate analysis, CD3+ T cell infiltration status was further evaluated according various staging systems—Ballantyne, modified Ballantyne, AJCC 8th cutaneous melanoma, and AJCC 8th colon and rectum

Fig. 5 Association of CD3+ T cells in invasion front and tumor stages according to various staging systems. The density of CD3+ T cell infiltration in invasion front was higher in lower stage groups than higher stage groups (mean \pm SD) by **a** Ballantyne staging system (stage I vs stages II–III, 334.0 ± 184.9 vs 182.0 ± 90.7 , $P = 0.016$), **b** Modified Ballantyne staging system (stage L vs stages R & D, 319.0 ± 176.4 vs 179.7 ± 93.6 , $P = 0.024$), and **d** AJCC colorectal staging system, stages I–II vs stages III–IV, 371.0 ± 177.3 vs 177.3 ± 87.9 , $P = 0.002$; Mann–Whitney U test). However, the density of CD3+ T cell infiltration in invasion front was tended to be different in lower stage groups than higher stage groups by **c** the AJCC cutaneous melanoma staging system (stages IIB–IIC vs stages III–IV, 340.0 ± 163.8 vs 205.8 ± 130.8 , $P = 0.089$).



staging systems (Fig. 5). The density of CD3+ T cell infiltration in IF was higher in lower stage groups than higher stage groups (mean \pm SD, Ballantyne stage I vs II–III, 334.0 ± 184.9 vs 182.0 ± 90.7 , $P = 0.016$, Fig. 5a; Modified Ballantyne stage L vs R & D, 319.0 ± 176.4 vs 179.7 ± 93.6 , $P = 0.024$, Fig. 5b; AJCC cutaneous melanoma stages IIB–IIC vs III–IV, 340.0 ± 163.8 vs 205.8 ± 130.8 , $P = 0.089$, Fig. 5c; AJCC colon and rectum stages I–II vs III–IV, 371.0 ± 177.3 vs 177.2 ± 87.9 , $P = 0.002$, Fig. 5d; Mann–Whitney U test).

The TIL infiltration patterns are associated with survival outcomes

The kappa values were 0.856 for Clark’s model and 0.783 for the tumor-immune phenotype, as found from the observations of the two experts, and showed moderate to good coincidence. A brisk infiltrate was observed in 31.8% of our current study cases. Significant survival difference was observed based on Clark’s model (overall comparison, $P = 0.0023$, Fig. 6a). Pair-wise comparisons revealed patients with ARMM having a brisk total TIL showed a better 3-year survival rate (3YSR, 85.7%) than those with a non-brisk TIL (55.6%, $P = 0.025$) or absent TIL (16.7%, $P = 0.002$, Fig. 6a). Similarly, significant survival difference was noted based on Clark’s model of CD3+ TIL

(overall comparison, $P = 0.0066$, Fig. 6b). Pair-wise comparisons revealed better OS was noted for patients with ARMM having a brisk (71.4%) compared to those with a non-brisk (62.5%, $P = 0.045$) or absent (28.5%, $P = 0.021$) CD3-positive TIL.

The immune phenotype was also found to be related to patient prognosis, and there was a significant difference in the OS (overall comparison, $P = 0.03$, Fig. 6c) and RFS (overall comparison, $P = 0.0038$, Fig. 6d) outcomes. An immune-inflamed tumor was observed in 27.3% of the study cases. Pair-wise comparisons revealed patients with ARMM having inflamed type had better OS (3YSR, 86.8%) and RFS (3YSR, 85.4%) than those with immune-excluded type (OS, 3YSR, 76.2% and RFS, 60.5%, $P = 0.045$ and $P = 0.03$, respectively). Patients with ARMM having immune-excluded type had better OS (3YSR, 76.2%) and RFS (3YSR, 60.5%) than those with immune-desert type (OS 3YSR, 27.1% and RFS 3YSR, 11.8%, $P = 0.028$ and $P = 0.023$, respectively, Fig. 6c, d).

Discussion

We observed differences in the immune profiles of patients with ARMM in accordance with the status of death and recurrence in these cases. Immune-related pathway scores

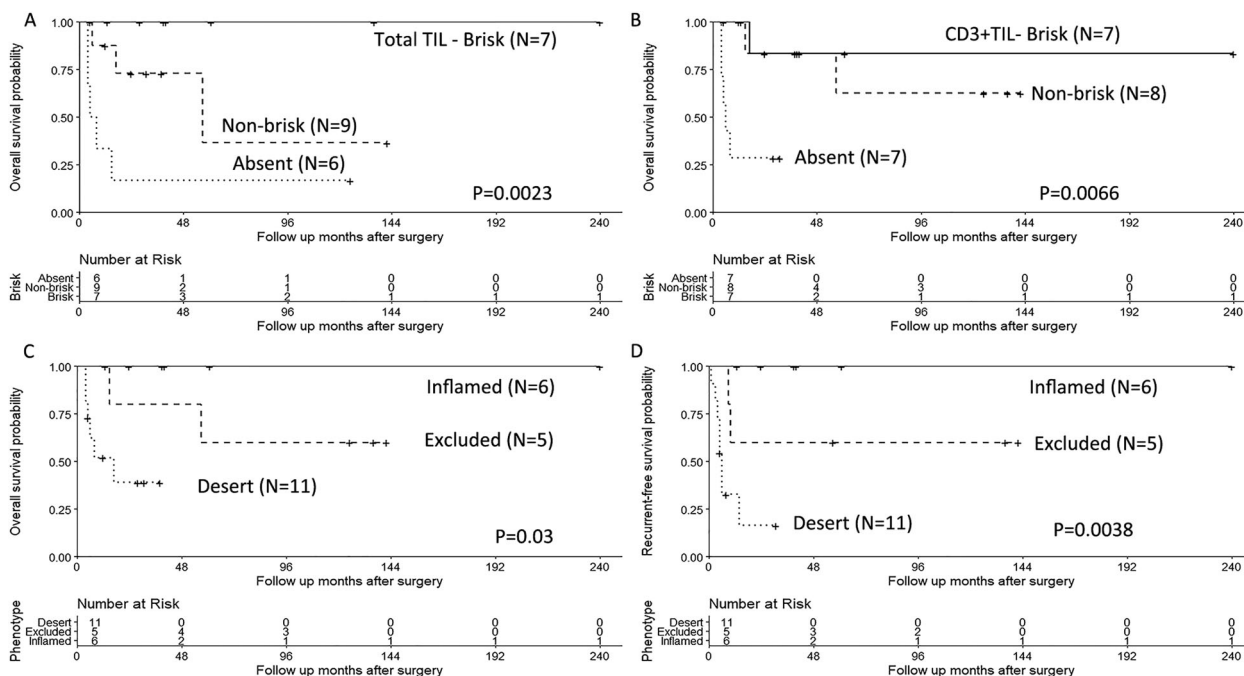


Fig. 6 Kaplan–Meier curves generated in accordance with the distribution patterns of immune cell infiltration in the study patients with anorectal malignant melanoma (ARMM). **a** Patients with a brisk total tumor infiltrating lymphocytes (TIL) (sum of CD3+, CD8+, and Foxp3+ T cell) show better overall survival (OS) rates

than those with a non-brisk TIL or absent TIL. **b** Patients with CD3+ TIL show better OS rates than those with a non-brisk TIL or absent TIL. **c, d** Patients with an inflamed phenotype have significantly better OS and recurrence free survival (RFS) rates than patients with an immune-desert and immune-excluded phenotype.

for mRNA data and for protein expression using IHC staining were all distinguishable between the recurrent and/or deceased and nonrecurrent and/or surviving patients with ARMM. A significant difference was observed when comparing the immune contexture scores between the two groups. Overall, the nonrecurrent and/or surviving ARMM cases had significantly higher immune contexture scores, suggesting that immune cell infiltration, such as the TIL and TAM, have an essential role in survival and recurrence in patients with ARMM. Furthermore, high-CD3+ T-cell infiltration at the IF was significantly associated with nonrecurrent and/or surviving patients, suggesting that it is an independent favorable prognostic indicator in patients with ARMM.

A prior study has also documented the effectiveness of TIL and PD-L1 as prognostic factors in ARMM, and demonstrated that a high TIL number and positive expression of PD-L1 in ARMM shows a trend toward improved survival [22]. However, this prior study by Dodds and colleagues did not focus on the survival outcomes of patients with ARMM with various complex immune contextures, and therefore, did not clearly describe any survival benefits. In our present study, we quantitatively and spatially analyzed the detailed relationship between the various immune cells in the patient's immune environment and their survival outcomes, using IHC. Furthermore, using mRNA analysis, we could observe differences between the

pathways associated with tumor growth and the immune cell-type profiling associated with the tumor microenvironment, depending on whether recurrences occurred or not. The pathway analysis exhibits the correlation of gene expression with the overall TIL score. The immune pathway scores showed high expression, which was correlated with an overall high TIL score in the nonrecurrent group when compared to the recurrent group having low gene expression and TIL scores. Our findings demonstrated that patients with nonrecurrent ARMM had significantly decreased scores in the pathways associated with tumor growth, and they also had a significantly higher immune score with respect to macrophages ($P = 0.05$), T-cell and B-cell profiles ($P < 0.01$) compared to patients with recurrent ARMM. IHC staining investigated the association of the TIL score with OS and prognosis. Our findings revealed that a high density of TIL was associated with favorable OS and prognosis in the nonrecurrent group than in the recurrent group with a low TIL density associated with poor OS and prognosis. In relation to NanoString analysis, we identified a high TIL expression score in the nonrecurrent group, which was the same as that of high TIL density in the IHC results. Likewise, low TIL expression scores in NanoString analysis were associated with low-density TIL in the IHC results. Therefore, NanoString analysis results were consistent with the IHC data on the basis of TIL scores. In addition, NanoString analysis results revealed the immune

pathways that are potentially responsible for differentiating the two tumor states.

There are difficulties in identifying factors that are relevant to the prognosis of ARMM owing to its rarity. Histopathological features associated with a poor prognosis in patients with ARMM include distant metastasis, increased invasion depth of the tumor, increased tumor size, and a positive resection margin [53, 54]. However, there is still some controversy regarding which factors have the most impact on ARMM prognosis. Ren et al. have studied a relatively large cohort with ARMMs ($N = 60$) and found that increased age (>70 years) and tumor extension beyond the deep muscular layer were negative prognostic indicators for survival [55]. In contrast, these authors have reported that lymph node metastasis, tumor thickness, and lympho-vascular and perineural invasion were not the prognostic factors [55]. Thus, a standardized universal staging system specific of ARMM is needed to be established. The latest (8th) edition of the AJCC staging system uses site specific staging schemes for malignancies in cutaneous malignant melanomas, conjunctival and uveal malignant melanomas, and mucosal malignant melanoma of the head and neck. However, ARMM was excluded from the anal tumor staging of this AJCC system [35]. Recently, a large study has reported that the tumor thickness of the 8th edition scheme of the AJCC staging system regarding cutaneous melanoma is meaningfully associated with prognostic significance in ARMM [25]. In the paper, the authors pointed out that a limitation of their study was that only six patients had a tumor thickness of <1.0 mm [25]. We observed that 82% of patients showing tumor thicknesses of >4.0 mm. In contrast, data on thin melanoma (tumor thickness <1.0 mm) is limited. The results of our present study were concurrent with those of the previous studies.

If predicting recurrence by immune profiling prior to patient treatment is clinically feasible, this may improve prognoses. The dynamic role of the adaptive immune response in cancer development, progression, and metastases has been reported in previous studies [56]. The NanoString gene expression panel has already been shown to be associated with pathway scores and histopathological factors in cutaneous malignant melanoma. These studies support the utilization of RNA expression in clinical practice to stratify patients according to clinically and biologically relevant scores. RNA expression data can be employed to calculate pathway scores more accurately, predict the responses to an immune checkpoint blockade prior to treatment, or be used during patient surveillance via relatively non-invasive mRNA profiling [57–60]. Recently, Gartrell et al. introduced melanoma immune profiles in a cohort of 78 patients with cutaneous malignant melanoma located in the neck and trunk [61]. The samples were subjected to RNA extraction regardless of tumor location, and

the NanoString assay was used to measure 53 target and 17 housekeeping genes. Immune profiling was linked to survival outcome and was found to be a useful tool to distinguish patients with distant metastatic recurrence from those without recurrence. Another study has suggested that adjuvant chemotherapy or immunotherapy can be spared for low-risk cases as predicted by their malignant melanoma immune profile [62]. Similarly, as adjuvant immunotherapy remains somewhat controversial owing to severe immune-related adverse events, our present study findings may contribute to better patient selection for immune checkpoint inhibitor treatment of ARMM after surgical resection.

To date, multiple studies have demonstrated that higher TIL infiltration is a favorable prognostic indicator in primary cutaneous malignant melanoma [61, 63, 64]. Various TIL grading systems have been proposed, but Clark's model remains the most commonly used grading system because of its simplicity and reproducibility [27]. We verified a significant difference in OS outcomes according to the TIL distribution pattern defined by the Clark's model in our current study series. In our present cohort, patients with ARMM having brisk TIL infiltration had the best survival rates and those with non-brisk infiltration had better OS outcomes than those without TIL infiltration. These results are consistent with those of a previous study on cutaneous malignant melanoma by Clark et al. Similarly, when ARMM was divided into three categories according to the immune phenotype, ARMM patients with an inflamed type had the best survival outcomes, and those with an excluded type had a better OS than those with the desert type. In this regard, a previous report has shown that cellular and molecular properties of immune phenotypes are pivotal determinants of both malignant melanoma progression and of therapeutic responses [51]. The results of our present study indicate that, as with cutaneous malignant melanoma, the location and infiltration pattern along with the TIL level are important prognostic determinants in ARMM [65, 66].

Recent work has shown that, apart from TIL density, the spatial location of immune cells is valuable in predicting patient prognosis [32]. Spatialization of lymphocytic infiltration in the context of nearby cancer cells is an important prognostic hallmark of certain types of tumors. This suggests that the study of the immune response with respect to patient outcome should be taken into account, and that this should include the quantity of immune cells as well as the spatialization among tumor cells and surrounding immune cells [20, 21, 23, 35]. In primary cutaneous melanoma, the prognostic value of TILs has been studied and many reports have established strict guidelines for defining 'TIL', stating that the lymphocytes must infiltrate and disrupt the tumor cell nests [5]. In our study, quantitative analysis revealed that the OS and RFS conferred significantly favorable prognoses when the TIL density was high (Fig. 4 and

Supplementary Fig. 9). Furthermore, in the context of spatialization, we found that most of the patients in the recurrent and/or deceased group had significantly lower immune cell infiltration into the intratumoral area, which confirmed the results of the previous report (Table 2). However, we also found that the stromal TIL was also significantly lower in the groups with patients with recurrent ARMM and/or deceased patients, and that the low stromal TIL was associated with a poor prognosis, which suggests the potential prognostic implication of stromal TILs in patients with ARMM. The tumor stroma, specifically, the stroma inside the borders of the invasive tumor, between the tumor nests, changes in relation to the adjacent stroma and has significant interactions with the tumor cells [33, 34]. We considered this stromal compartment to be an essential part of the tumor, and therefore, we suggest that stromal TILs should also be evaluated.

We quantified the composition of various immune cells and evaluated their survival benefit in our ARMM cohort. Notably, high densities of TILs [pan-T cells, cytotoxic T cells, regulatory T cells (Treg)] and TAMs (CD68 and CD163)] were found to be associated with a favorable prognosis in patients with ARMM, whether they were at the IF or in the TC. Our results indicated that if TILs and TAMs show plentiful infiltration, they play an important role in antitumor immunity. Of note, in multivariate analysis, CD3+ T-cell infiltration at the IF was an important independent prognostic factor in the present study, which indicated the potential importance of peritumoral TILs. A recent study has shown that the TIL density at the invasion margin was able to consistently predict responses to immune checkpoint inhibitor therapy, with pembrolizumab performing better than CD8+ T-cell density within the tumor and better than CD4+, PD-1+, and PD-L1+ T-cell densities within the tumor or at the invasive margin [67]. The data of this study agree with our data and have helped in renewing interest in the potential use of peritumoral TILs as a reliable biomarker to predict responses to immune checkpoint inhibitor therapy.

Treg are the main cell population involved in maintaining peripheral tolerance [68]. The most specific Treg marker, Foxp3, has been shown to correlate with a poor prognosis in various types of human cancers [69–71]. However, most previous studies on malignant melanoma have suggested that Foxp3+ T cells are associated with a favorable prognosis [72, 73]. In our study, Foxp3+ Treg also show favorable prognostic role in ARMM. To clarify the antitumor role of Treg, the ratios of Foxp3+ Treg to other lymphocyte subsets were calculated, which was reported as a potentially effective indicator of quantifying Treg [69]. However, the ratios of Foxp3+ Treg to other lymphocytes subset also showed favorable prognosis in the

present study. Further studies are required to clarify the mechanisms involving Treg in ARMMs.

Our present study investigated the effectiveness of assessing TILs in patients with ARMM in terms of their localization, expression, and distribution patterns associated with survival outcomes. Our results provide new and important insights into the appropriate follow-up strategies and approaches to predict prognoses in patients with ARMM. Our current study also had a few limitations, including its retrospective single-center design and small case numbers owing to the rarity of the disease. In addition, the number of patients who received any form of immunotherapy in our cohort was very small ($N=2$), thus preventing any meaningful comparisons between pre- and post-immunotherapy cases. Therefore, future studies of ARMM should include larger patient cohorts that have received immunotherapy with external validation, as well as follow-up data on the responses to these treatments.

In conclusion, we showed that patients with ARMM have a more favorable OS and RFS in cases with a higher density of TILs, including CD3+, CD8+, and Foxp3+ T cells. In addition, the presence of CD3+ TILs at the IF was an independent favorable prognostic indicator in patients with ARMM. Consideration of the TIL distribution pattern/infiltration phenotype in ARMM and identifying patients who demonstrate an immune-inflamed phenotype and brisk-infiltration patterns is crucial for making an accurate prognostic stratification and guiding treatment approaches.

Acknowledgements This research was supported by a grant of the Asan Institute for Life Sciences, Asan Medical Center, Seoul, Republic of Korea [grant number: 2016-729].

Compliance with ethical standards

Conflict of interest The authors declare that they have no conflict of interest.

Publisher's note Springer Nature remains neutral with regard to jurisdictional claims in published maps and institutional affiliations.

References

- Schaefer T, Satzger I, Gutzmer R. Clinics, prognosis and new therapeutic options in patients with mucosal melanoma: a retrospective analysis of 75 patients. *Medicine*. 2017;96:e5753.
- Malaguarnera G, Madeddu R, Catania VE, Bertino G, Morelli L, Perrotta RE, et al. Anorectal mucosal melanoma. *Oncotarget*. 2018;9:8785–800.
- Hillenbrand A, Barth TF, Henne-Bruns D, Formentini A. Anorectal amelanotic melanoma. *Colorectal Dis*. 2008;10:612–5.
- Brady MS, Kavolius JP, Quan SH. Anorectal melanoma. A 64-year experience at Memorial Sloan-Kettering Cancer Center. *Dis Colon Rectum*. 1995;38:146–51.
- Furney SJ, Turajlic S, Stamp G, Nohadani M, Carlisle A, Thomas JM, et al. Genome sequencing of mucosal melanomas reveals that

- they are driven by distinct mechanisms from cutaneous melanoma. *J Pathol.* 2013;230:261–9.
6. Hayward NK, Wilmott JS, Waddell N, Johansson PA, Field MA, Nones K, et al. Whole-genome landscapes of major melanoma subtypes. *Nature.* 2017;545:175–80.
 7. Krauthammer M, Kong Y, Ha BH, Evans P, Bacchicocchi A, McCusker JP, et al. Exome sequencing identifies recurrent somatic RAC1 mutations in melanoma. *Nat Genet.* 2012;44:1006–14.
 8. Helmke BM, Mollenhauer J, Herold-Mende C, Benner A, Thome M, Gassler N, et al. BRAF mutations distinguish anorectal from cutaneous melanoma at the molecular level. *Gastroenterology.* 2004;127:1815–20.
 9. Cohen Y, Rosenbaum E, Begum S, Goldenberg D, Esche C, Lavie O, et al. Exon 15 BRAF mutations are uncommon in melanomas arising in nonsun-exposed sites. *Clin Cancer Res.* 2004;10:3444–7.
 10. Edwards RH, Ward MR, Wu H, Medina CA, Brose MS, Volpe P, et al. Absence of BRAF mutations in UV-protected mucosal melanomas. *J Med Genet.* 2004;41:270–2.
 11. Maldonado JL, Fridlyand J, Patel H, Jain AN, Busam K, Kageshita T, et al. Determinants of BRAF mutations in primary melanomas. *J Natl Cancer Inst.* 2003;95:1878–90.
 12. Wellbrock C, Hurlstone A. BRAF as therapeutic target in melanoma. *Biochem Pharmacol.* 2010;80:561–7.
 13. Long GV, Menzies AM, Nagrial AM, Haydu LE, Hamilton AL, Mann GJ, et al. Prognostic and clinicopathologic associations of oncogenic BRAF in metastatic melanoma. *J Clin Oncol.* 2011;29:1239–46.
 14. Schadendorf D, Hodi FS, Robert C, Weber JS, Margolin K, Hamid O, et al. Pooled analysis of long-term survival data from Phase II and Phase III trials of ipilimumab in unresectable or metastatic melanoma. *J Clin Oncol.* 2015;33:1889–94.
 15. Taylor JP, Stem M, Yu D, Chen SY, Fang SH, Gearhart SL, et al. Treatment strategies and survival trends for anorectal melanoma: is it time for a change? *World J Surg.* 2019;43:1809–19.
 16. Ciarrocchi A, Pietroletti R, Carlei F, Amicucci G. Extensive surgery and lymphadenectomy do not improve survival in primary melanoma of the anorectum: results from analysis of a large database (SEER). *Colorectal Dis.* 2017;19:158–64.
 17. Tyrrell H, Payne M. Combatting mucosal melanoma: recent advances and future perspectives. *Melanoma Manag.* 2018;5: Mmt11.
 18. D'Angelo SP, Larkin J, Sosman JA, Lebbe C, Brady B, Neyns B, et al. Efficacy and safety of nivolumab alone or in combination with ipilimumab in patients with mucosal melanoma: a pooled analysis. *J Clin Oncol.* 2017;35:226–35.
 19. Yentz S, Lao CD. Immunotherapy for mucosal melanoma. *Ann Transl Med.* 2019;7:S118.
 20. Moya-Plana A, Herrera Gomez RG, Rossoni C, Dercle L, Ammari S, Girault I, et al. Evaluation of the efficacy of immunotherapy for non-resectable mucosal melanoma. *Cancer Immunol Immunother.* 2019;68:1171–8.
 21. Kaunitz GJ, Cottrell TR, Lilo M, Muthappan V, Esandrio J, Berry S, et al. Melanoma subtypes demonstrate distinct PD-L1 expression profiles. *Lab Invest.* 2017;97:1063–71.
 22. Dodds TJ, Wilmott JS, Jackett LA, Lo SN, Long GV, Thompson JF, et al. Primary anorectal melanoma: clinical, immunohistology and DNA analysis of 43 cases. *Pathology.* 2019;51:39–45.
 23. Bello DM, Smyth E, Perez D, Khan S, Temple LK, Ariyan CE, et al. Anal versus rectal melanoma: does site of origin predict outcome? *Dis Colon Rectum.* 2013;56:150–7.
 24. SE M. *Histology for pathologists.* 4th ed. Philadelphia: Lippincott Williams & Wilkins; 2012.
 25. Nagarajan P, Piao J, Ning J, Noordenbos LE, Curry JL, Torres-Cabala CA, et al. Prognostic model for patient survival in primary anorectal mucosal melanoma: stage at presentation determines relevance of histopathologic features. *Mod Pathol.* 2020;33:496–513.
 26. Breslow A. Prognosis in cutaneous melanoma: tumor thickness as a guide to treatment. *Pathol Annu.* 1980;15:1–22.
 27. Clark WH Jr., Elder DE, Guerry Dt, Braitman LE, Trock BJ, Schultz D, et al. Model predicting survival in stage I melanoma based on tumor progression. *J Natl Cancer Inst.* 1989;81:1893–904.
 28. Thompson JF, Soong SJ, Balch CM, Gershenwald JE, Ding S, Coit DG, et al. Prognostic significance of mitotic rate in localized primary cutaneous melanoma: an analysis of patients in the multi-institutional American Joint Committee on Cancer melanoma staging database. *J Clin Oncol.* 2011;29:2199–205.
 29. Tetzlaff MT, Curry JL, Ivan D, Wang WL, Torres-Cabala CA, Bassett RL, et al. Immunodetection of phosphohistone H3 as a surrogate of mitotic figure count and clinical outcome in cutaneous melanoma. *Mod Pathol.* 2013;26:1153–60.
 30. Grande Sarpa H, Reinke K, Shaikh L, Leong SP, Miller JR 3rd, Sagebiel RW, et al. Prognostic significance of extent of ulceration in primary cutaneous melanoma. *Am J Surg Pathol.* 2006;30:1396–1400.
 31. Kashani-Sabet M, Sagebiel RW, Ferreira CM, Nosrati M, Miller JR 3rd. Vascular involvement in the prognosis of primary cutaneous melanoma. *Arch Dermatol.* 2001;137:1169–73.
 32. Baer SC, Schultz D, Synnestvedt M, Elder DE. Desmoplasia and neurotropism. Prognostic variables in patients with stage I melanoma. *Cancer.* 1995;76:2242–7.
 33. Schatton T, Scolyer RA, Thompson JF, Mihm MC Jr. Tumor-infiltrating lymphocytes and their significance in melanoma prognosis. *Methods Mol Biol.* 2014;1102:287–324.
 34. Bosman FT CF, Hruban RH, Theise ND. WHO classification of tumours of the digestive system. Lyon: The International Agency for Research on Cancer; 2018.
 35. Amin MB, Edge SB, American Joint Committee on C. *AJCC cancer staging manual.* 8th ed. New York, NY: Springer; 2017.
 36. Ballantyne AJ. Malignant melanoma of the skin of the head and neck. An analysis of 405 cases. *Am J Surg.* 1970;120:425–31.
 37. Boger C, Behrens HM, Mathiak M, Kruger S, Kalthoff H, Rocken C. PD-L1 is an independent prognostic predictor in gastric cancer of Western patients. *Oncotarget.* 2016;7:24269–83.
 38. Delgado J, Pereira A, Villamor N, López-Guillermo A, Rozman C. Survival analysis in hematologic malignancies: recommendations for clinicians. *Haematologica.* 2014;99:1410–20.
 39. Seckinger A, Meissner T, Moreaux J, Depeweg D, Hillengass J, Hose K, et al. Clinical and prognostic role of annexin A2 in multiple myeloma. *Blood.* 2012;120:1087–94.
 40. Kassambara A, Gourzones-Dmitriev C, Sahota S, Reme T, Moreaux J, Goldschmidt H, et al. A DNA repair pathway score predicts survival in human multiple myeloma: the potential for therapeutic strategy. *Oncotarget.* 2014;5:2487–98.
 41. Hassen W, Kassambara A, Reme T, Sahota S, Seckinger A, Vincent L, et al. Drug metabolism and clearance system in tumor cells of patients with multiple myeloma. *Oncotarget.* 2015;6:6431–47.
 42. Bailly C, Carlier T, Jamet B, Eugene T, Touzeau C, Attal M, et al. Interim PET analysis in first-line therapy of multiple myeloma: prognostic value of DeltaSUVmax in the FDG-Avid Patients of the IMAJEM Study. *Clin Cancer Res.* 2018;24:5219–24.
 43. Park SY, Cho A, Yu WS, Lee CY, Lee JG, Kim DJ, et al. Prognostic value of total lesion glycolysis by 18F-FDG PET/CT in surgically resected stage IA non-small cell lung cancer. *J Nucl Med.* 2015;56:45–9.
 44. Lee HJ, Lee JJ, Park JY, Kim JH, Kim YM, Kim YT, et al. Prognostic value of metabolic parameters determined by

- preoperative (1)(8)F-FDG PET/CT in patients with uterine carcinosarcoma. *J Gynecol Oncol.* 2017;28:e43.
45. Jeong Y, Baek S, Park JW, Joo JH, Kim JS, Lee SW. Lymph node standardized uptake values at pre-treatment (18)F-fluorodeoxyglucose positron emission tomography as a valuable prognostic factor for distant metastasis in nasopharyngeal carcinoma. *Br J Radiol.* 2017;90:20160239.
 46. Choi YH, Lee SH, You MS, Shin BS, Paik WH, Ryu JK, et al. Prognostic factors for patients with borderline resectable or locally advanced pancreatic cancer receiving Neoadjuvant FOLFIRINOX. *Gut Liver.* 2020. [Online ahead of print].
 47. Lotem M, Merims S, Frank S, Hamburger T, Nissan A, Kadouri L, et al. Adjuvant autologous melanoma vaccine for macroscopic Stage III disease: survival, biomarkers, and improved response to CTLA-4 Blockade. *J Immunol Res.* 2016;2016:8121985–8121985.
 48. Zeng D, Li M, Zhou R, Zhang J, Sun H, Shi M, et al. Tumor microenvironment characterization in gastric cancer identifies prognostic and immunotherapeutically relevant gene signatures. *Cancer Immunol Res.* 2019;7:737–50.
 49. Hothorn T, Lausen B. Maxstat: maximally selected rank statistics. R package version 07-21; 2015.
 50. Clemente CG, Mihm MC Jr, Bufalino R, Zurrida S, Collini P, Cascinelli N. Prognostic value of tumor infiltrating lymphocytes in the vertical growth phase of primary cutaneous melanoma. *Cancer.* 1996;77:1303–10.
 51. Chen DS, Mellman I. Elements of cancer immunity and the cancer-immune set point. *Nature.* 2017;541:321–30.
 52. Lanitis E, Dangaj D, Irving M, Coukos G. Mechanisms regulating T-cell infiltration and activity in solid tumors. *Ann Oncol.* 2017;28:xii18–xii32.
 53. Nam S, Kim CW, Baek SJ, Hur H, Min BS, Baik SH, et al. The clinical features and optimal treatment of anorectal malignant melanoma. *Ann Surg Treat Res.* 2014;87:113–7.
 54. Weinstock MA. Epidemiology and prognosis of anorectal melanoma. *Gastroenterology.* 1993;104:174–8.
 55. Ren M, Lu Y, Lv J, Shen X, Kong J, Dai B, et al. Prognostic factors in primary anorectal melanoma: a clinicopathological study of 60 cases in China. *Hum Pathol.* 2018;79:77–85.
 56. Mittal D, Gubin MM, Schreiber RD, Smyth MJ. New insights into cancer immunoediting and its three component phases—elimination, equilibrium and escape. *Curr Opin Immunol.* 2014;27:16–25.
 57. Kwong LN, De Macedo MP, Haydu L, Joon AY, Tetzlaff MT, Calderone TL, et al. Biological validation of RNA sequencing data from formalin-fixed paraffin-embedded primary melanomas. *JCO Prec Oncol.* 2018. <https://doi.org/10.1200/PO.1217.00259>.
 58. Jiang P, Gu S, Pan D, Fu J, Sahu A, Hu X, et al. Signatures of T cell dysfunction and exclusion predict cancer immunotherapy response. *Nat Med.* 2018;24:1550–8.
 59. Latchana N, DiVincenzo MJ, Regan K, Abrams Z, Zhang X, Jacob NK, et al. Alterations in patient plasma microRNA expression profiles following resection of metastatic melanoma. *J Surg Oncol.* 2018;118:501–9.
 60. Buart S, Terry S, Noman MZ, Lanoy E, Boutros C, Fogel P, et al. Transcriptional response to hypoxic stress in melanoma and prognostic potential of GBE1 and BNIP3. *Oncotarget.* 2017;8:108786–801.
 61. Gartrell RD, Marks DK, Hart TD, Li G, Davari DR, Wu A, et al. Quantitative analysis of immune infiltrates in primary melanoma. *Cancer Immunol Res.* 2018;6:481–93.
 62. Gartrell RD, Marks DK, Rizk EM, Bogardus M, Gerard CL, Barker LW, et al. Validation of Melanoma Immune Profile (MIP), a prognostic immune gene prediction score for Stage II-III melanoma. *Clin Cancer Res.* 2019;25:2494–502.
 63. Azimi F, Scolyer RA, Rumcheva P, Moncrieff M, Murali R, McCarthy SW, et al. Tumor-infiltrating lymphocyte grade is an independent predictor of sentinel lymph node status and survival in patients with cutaneous melanoma. *J Clin Oncol.* 2012;30:2678–83.
 64. Gajewski TF, Schreiber H, Fu YX. Innate and adaptive immune cells in the tumor microenvironment. *Nat Immunol.* 2013;14:1014–22.
 65. Tucci M, Passarelli A, Mannavola F, Felici C, Stucci LS, Cives M, et al. Immune system evasion as Hallmark of melanoma progression: the role of dendritic cells. *Front Oncol.* 2019;9:1148.
 66. Kather JN, Suarez-Carmona M, Charoentong P, Weis CA, Hirsch D, Bankhead P, et al. Topography of cancer-associated immune cells in human solid tumors. *Elife.* 2018;7:e36967.
 67. Hendry S, Salgado R, Gevaert T, Russell PA, John T, Thapa B, et al. Assessing tumor infiltrating lymphocytes in solid tumors: a practical review for pathologists and proposal for a standardized method from the International Immuno-Oncology Biomarkers Working Group: Part 2: TILs in melanoma, gastrointestinal tract carcinomas, non-small cell lung carcinoma and mesothelioma, endometrial and ovarian carcinomas, squamous cell carcinoma of the head and neck, genitourinary carcinomas, and primary brain tumors. *Adv Anat Pathol.* 2017;24:311.
 68. Sakaguchi S, Yamaguchi T, Nomura T, Ono M. Regulatory T cells and immune tolerance. *Cell.* 2008;133:775–87.
 69. Fu Q, Chen N, Ge C, Li R, Li Z, Zeng B, et al. Prognostic value of tumor-infiltrating lymphocytes in melanoma: a systematic review and meta-analysis. *Oncoimmunology.* 2019;8:1593806.
 70. Mougiakakos D, Johansson CC, Trocme E, All-Ericsson C, Economou MA, Larsson O, et al. Intratumoral forkhead box P3-positive regulatory T cells predict poor survival in cyclooxygenase-2-positive uveal melanoma. *Cancer.* 2010;116:2224–33.
 71. Lagouros E, Salomao D, Thorland E, Hodge DO, Vile R, Pulido JS. Infiltrative T regulatory cells in enucleated uveal melanomas. *Trans Am Ophthalmol Soc.* 2009;107:223–8.
 72. Knol AC, Nguyen JM, Quereux G, Brocard A, Khammari A, Dreno B. Prognostic value of tumor-infiltrating Foxp3+ T-cell subpopulations in metastatic melanoma. *Exp Dermatol.* 2011;20:430–4.
 73. Balatoni T, Mohos A, Papp E, Sebestyen T, Liskay G, Olah J, et al. Tumor-infiltrating immune cells as potential biomarkers predicting response to treatment and survival in patients with metastatic melanoma receiving ipilimumab therapy. *Cancer Immunol Immunother.* 2018;67:141–51.